Figure 1. Effects of heat shock protein 60 (HSP60) on HBcAg-specific interleukin 10 (IL-10)–secreting regulatory T (T_{reg}) cells. *A*, Flow chart of the methods. *B*, Representative dot plots of IL-10-secreting cells in the CD4$^+$CD25$^+$ cells. The mixed cells (antigen-presenting cells [APCs; CD4$^-$] and isolated CD4$^+$CD25$^+$ cells) were stained with anti-CD4–peridinin chlorophyll protein complex (PerCP), anti-CD25–fluorescein isothiocyanate (FITC), and anti-IL-10-phycoerythrin (PE). The numbers in each top right quadrant indicate the frequencies of CD25$^+$ IL-10-secreting cells among the CD4$^+$ cells. The numbers in each bottom right quadrant indicate the frequencies of CD4$^+$CD25$^+$IL-10$^-$ cells among the CD4$^+$ cells. The numbers in each box in the top right quadrant indicate the frequencies of CD25$^+$ IL-10-secreting cells among the CD4$^+$ cells. *C*, Representative results for a sample from 1 patient with chronic hepatitis B (samples were obtained from 3 patients with chronic hepatitis B; this experiment was repeated 3 times). Bars indicate the percentage of IL-10-secreting cells among the CD4$^+$ cells with various kinds of pretreatment. *D*, Percentage of high–IL-10-secreting cells among the CD4$^+$ cells. Error bars indicate the standard deviation of 3 independent experiments with a sample from 1 patient with chronic hepatitis B. Three independent experiments yielded similar results to those shown in panels *C* and *D*. *$P < .05$.

Figure 2. Effect of recombinant heat shock protein 60 (rHSP60) on the interleukin 10 (IL-10)–secreting activity of CD4+CD25+ cells.

system (Roche). ELISA kits were used to assay HBsAg (Hope Laboratories) and HBeAg (BioChain Institute) in 50 μL of the culture supernatant.

Sequence analysis of HBV DNA. The presence of HBV DNA in the serum samples was determined by means of PCR, as described elsewhere [30]. Nucleic acids were extracted from 100 mL of serum and subjected to nested PCR for the S gene. The amplification product of the first-round PCR was 461 bp, and that of the second-round PCR was 437 bp. The amplification products were sequenced directly on both strands by use of the BigDye Terminator Cycle Sequencing Ready reaction kit on an ABI Prism 3100 genetic analyzer (Applied Biosystems).

Carboxyfluorescein succinimidyl ester (CFSE) staining and suppression assay. The suppressive activity of regulatory T cells was analyzed by use of a CellTrace CFSE cell proliferation kit (Molecular Probes). Staining methods were followed according to the manufacturer's protocol. Briefly, the collected CD4+CD25− cells were washed and resuspended in prewarmed phosphate-buffered saline with 0.1% bovine serum albumin at a final concentration of 3×10^5 cells/mL. CFSE solution (5 μm) was added and incubated at 37°C for 10 min. Stained cells were washed 3 times and incubated with unstained CD4+CD25+ T$_{reg}$ cells and CD3CD28-coated stimulation beads (T cell expander) for an additional 3 d. The cells were analyzed by means flow cytometry with 488-nm excitation and emission filters.

Statistics. The data in Figures 3, 4, 1C, 1D, and 5 were analyzed by use of the independent t test. Statistical correlation analysis of the data in Figure 6 was performed by use of the Kendall τ_b test. The data in Figure 7 were analyzed by use of the Wilcoxon rank sum test. All of the statistical analyses were performed with SPSS software (version 10.0; SPSS). Results for which $P < .05$ were considered to be statistically significant.

RESULTS

Levels of sHSP60 and sHSP70 in samples from HBeAg-positive patients with chronic hepatitis B, HBeAg-negative patients with chronic hepatitis B, and control patients with chronic hepatitis C. The patients' characteristics, including age, sex, and ALT level, were matched among the different patient groups because the levels of sHSP60 and sHSP70 might be influenced by these factors (Table 1). The mean ($\pm$ standard deviation [SD]) serum level of sHSP60 was 5.77 $\pm$ 1.19 ng/mL in HBeAg-positive patients with chronic hepatitis B, 4.12 $\pm$ 1.37 ng/mL in HBeAg-negative patients with chronic hepatitis B, 2.11 $\pm$

0.96 ng/mL in patients with chronic hepatitis C, and 0.54 $\pm$ 0.46 ng/mL in healthy subjects. The levels of sHSP60 in patients with chronic hepatitis B (HBeAg-positive and HBeAg-negative) were statistically significantly higher than those in patients with chronic hepatitis C (Figure 3). On the other hand, the mean ($\pm$ SD) serum level of sHSP70 was 7.89 $\pm$ 3.51 ng/mL in HBeAg-positive patients with chronic hepatitis B, 7.73 $\pm$ 3.71 ng/mL in HBeAg-negative patients with chronic hepatitis B, 8.09 $\pm$ 3.64 ng/mL in patients with chronic hepatitis C, and 3.54 $\pm$ 0.46 ng/mL in healthy subjects. There were no statistically significant differences in the level of sHSP70 between the chronic hepatitis B and chronic hepatitis C patient groups (Figure 3). Then we examined the correlations between the HSP60, HSP70, and HBV DNA or ALT levels. The levels of sHSP60 were correlated with the HBV DNA levels ($r = 0.532$; $P < .001$) but not with the ALT levels ($r = 0.101$; $P = .315$) (Figures 6A and 6B). On the other hand, the levels of sHSP70 were correlated with the ALT levels ($r = 0.520$; $P < .001$) but not with the HBV DNA levels ($r = 0.076$; $P < .449$) (Figure 6C and 6D).

HBV replication could directly induce sHSP60 production in vitro. Two kinds of plasmids carrying a 1.3-fold HBV genome that could replicate in HepG2 cells were used to analyze whether HBV replication could affect the production of sHSP60 in culture medium. The transfection efficiency was almost the
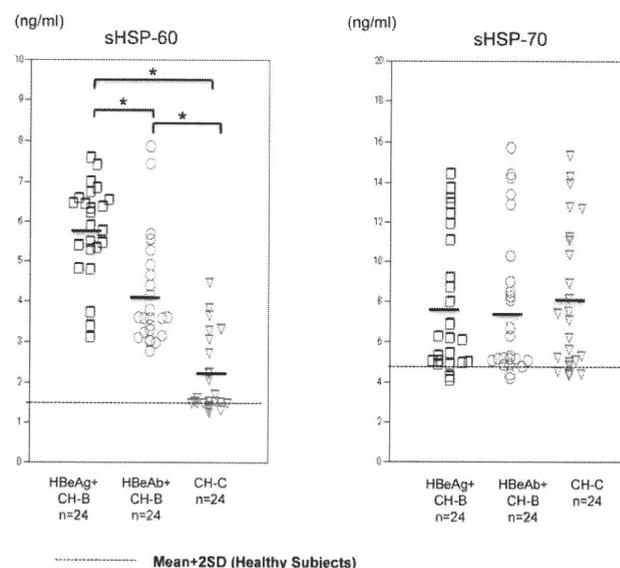
Figure 3. Quantification of serum levels of heat shock protein 60 (HSP60) and heat shock protein 70 (HSP70) in HBeAg-positive patients with chronic hepatitis B (CH-B), HBeAb-positive patients with CH-B, and patients with chronic hepatitis C (CH-C). Serum levels of HSP60 and HSP70 were quantified by means of enzyme-linked immunosorbent assay. The bar represents the means of the levels of HSP60 and HSP70. Dotted lines indicate the mean value plus 2 times the standard deviation (SD) of the levels of healthy subjects.
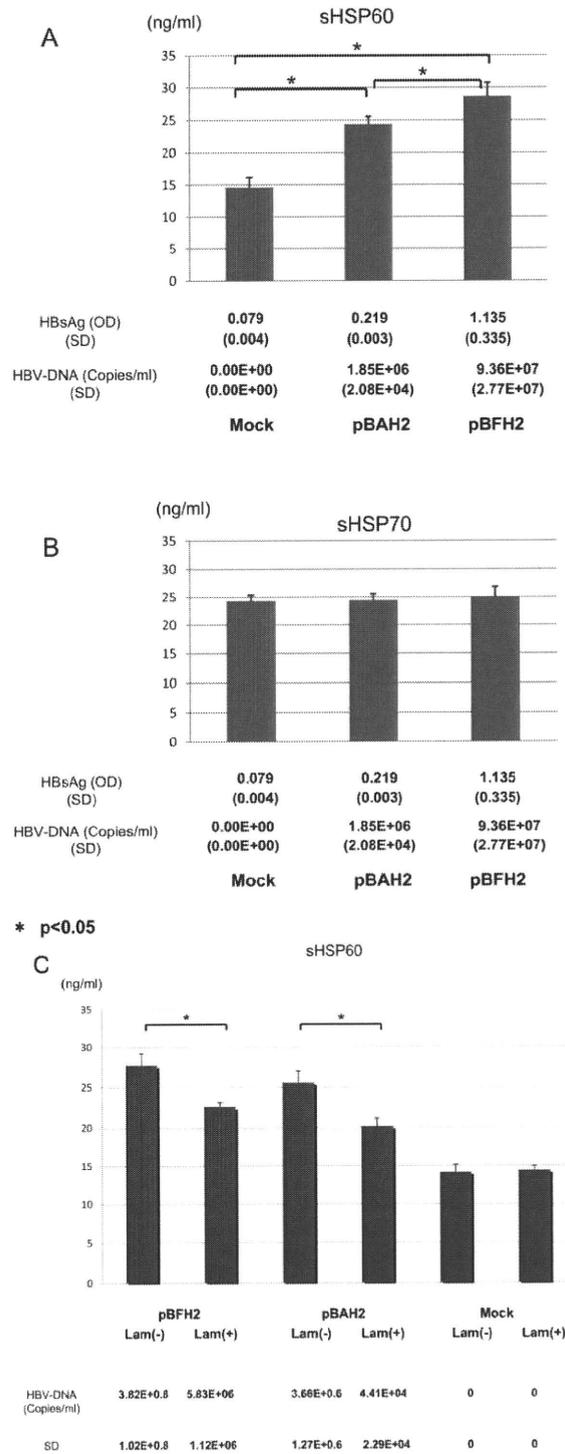
Figure 4. Direct effect of hepatitis B virus (HBV) on the production of heat shock protein 60 (HSP60) and heat shock protein 70 (HSP70). Two kinds of plasmid (pBAH2 and pBFH2) carrying a 1.3-fold HBV genome that could replicate in HepG2 cells and a mock plasmid were used to analyze whether HBV replication affects the production of soluble HSP60 (sHSP60) in culture medium. The levels of sHSP60 and soluble HSP70 (sHSP70) were compared among the 3 plasmid groups. Bars indicate the levels of HSP60 (*A*) and HSP70 (*B*). The HBsAg and HBV DNA levels and standard deviations (SDs) are included below the bar graphs. *C,* Levels of sHSP60 in cells with and those in cells without lamivudine treatment. The cells were treated with lamivudine (Lam; 0.5 μmol/L) for 72 h. Three independent experiments were performed.
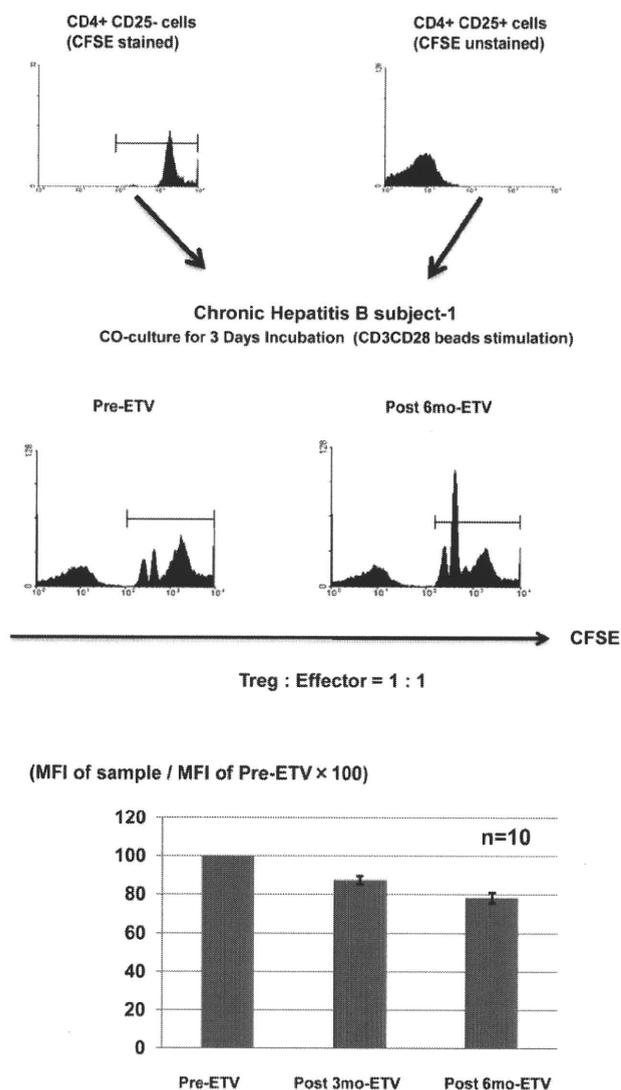
Figure 5. Suppression assay of regulatory T (T$_{reg}$) cells. The suppressive activity of T$_{reg}$ cells was analyzed by means of coincubation of unstained isolated T$_{reg}$ cells and autologous CD4$^+$CD25$^-$ cells with carboxyfluorescein succinimidyl ester (CFSE) staining. *A*, Representative histogram of CFSE-stained CD4$^+$CD25$^-$ effector cells and unstained CD4$^+$CD25$^+$ T$_{reg}$ cells. *B*, Various levels of cell division in CD4$^+$CD25$^-$ effector cells observed 3 d after coincubation with CD3CD28-coated beads. *C*, Mean fluorescence intensity (MFI) of CFSE staining of CD4$^+$CD25$^-$ cells before treatment, 3 months after the start of entecavir (ETV) treatment, and 6 months after the start of entecavir treatment. The bars show the MFI of the samples divided by the MFI of the pretreatment samples ×100. The error bars indicate the standard deviations of the data.

same among the different plasmids (data not shown). The mean (± SD) HBV DNA levels of pBAH2 and pBFH2 were $1.85 \times 10^6 \pm 2.08 \times 10^4$ and $9.36 \times 10^7 \pm 2.77 \times 10^7$ copies/mL, respectively. The levels of sHSP60 in the supernatant of the pBAH2- and pBFH2-transfected HepG2 cells were statistically significantly higher than that of the mock-transfected HepG2 cells ($P < .05$) (Figure 4*A*). However, the levels of

sHSP70 in the supernatant of the pBAH2- and pBFH2-transfected HepG2 cells were comparable with that of the mock-transfected HepG2 cells (Figure 4*B*). The addition of HBV-derived antigen in the culture supernatant could not increase the level of sHSP60 (data not shown). We performed the experiment on the suppression of HBV replication by nucleoside analogues in vitro. The suppression of HBV replication could statistically significantly reduce the production of sHSP60 (Figure 4*C*). These data indicate that HBV replication could increase the level of sHSP60 in the supernatant of the hepatocyte culture.

The effect of HSP60 on the HBcAg-specific IL-10-secreting T$_{reg}$ cells. Previously, we found that HBcAg-specific IL-10-secreting cells could play an important role in the hyporesponsiveness of T cells in patients with chronic hepatitis B [9]. The effects of HSP60 on HBcAg-specific IL-10-secreting T$_{reg}$ cells were analyzed. The appropriate dose of rHSP60 pretreatment was determined by use of PBMCs from healthy subjects (Figure 2). Pretreatment with rHSP60 could increase the frequency of HBcAg-specific IL-10-secreting cells statistically significantly ($P < .01$) and enhance the function of IL-10 secretion of HBcAg-specific T$_{reg}$ cells, because the frequencies of high-intensity cells with IL-10 staining in HSP60 pretreatment T$_{reg}$ cells were statistically significantly higher than those of control groups (Figure 1*D*). Moreover, these effects were completely blocked by neutralizing TLR2 antibody but not by TLR4 antibody. These data indicate that HSP60 might enhance the susceptibility and function of IL-10 secretion of HBcAg-specific T$_{reg}$ cells.

Sequential analysis of clinical samples collected during entecavir therapy. Ten patients were selected for sequential analysis during entecavir therapy. The titers of HBV DNA and the ALT level rapidly decreased during entecavir therapy (Figures 7*A* and 7*B*). The serum levels of HSP60 had statistically significantly decreased at 3 months and at 6 months after the start of entecavir therapy. The frequency of T$_{reg}$ cells and the expression level of TLR2 during entecavir treatment were quantified sequentially for up to 6 months during treatment by means of flow cytometry analysis. The frequency of CD4$^+$CD25$^+$ cells decreased, although not statistically significantly. On the other hand, the frequency of CD4$^+$CD25$^+$IL7R$^-$ cells (subpopulation of CD4$^+$CD25$^+$ cells) had statistically significantly decreased at 3 months and at 6 months after the start of entecavir therapy. The reason for the discrepancy could be that CD4$^+$CD25$^+$ cells included not only T$_{reg}$ cells but also activated CD4$^+$ effector cells. Previously, some research groups had found that CD4$^+$CD25$^+$FoxP3$^+$ cells are almost the same as CD4$^+$CD25$^+$IL7R$^-$ cells. Therefore, our data indicate that entecavir therapy could reduce the frequency of T$_{reg}$ cells. We also investigated the frequency of CD4$^+$CD25$^+$FoxP3$^+$ cells during lamivudine therapy (Figure 8). The frequency of
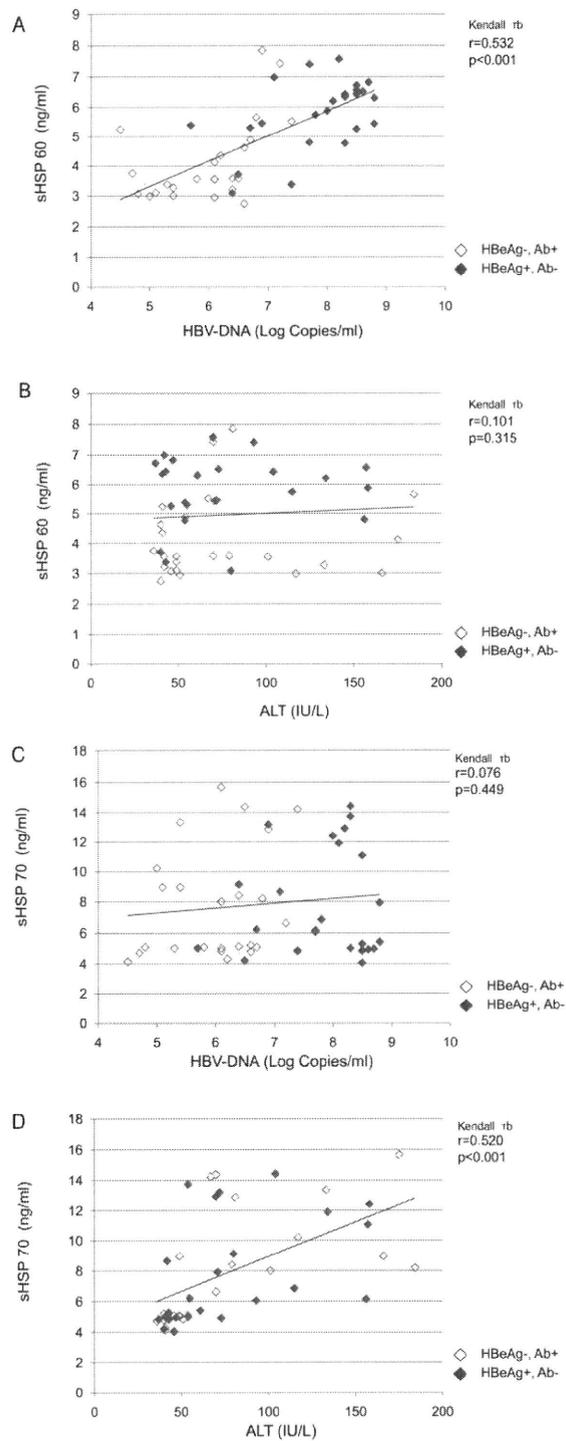
Figure 6. Analysis of the correlations between levels of heat shock proteins (HSPs), hepatitis B virus (HBV) DNA, and alanine aminotransferase (ALT). Open symbols indicate the values in samples from HBeAg-negative, HBeAb-positive patients. Filled symbols indicate the values in samples from HBeAg-positive, HBeAb-negative patients. The statistical analysis was performed by use of nonparametric Kendall τ_b methods. An approximately straight line is included in each graph. *A,* Correlation between heat shock protein 60 (HSP60) level and HBV DNA level. *B,* Correlation between HSP60 level and ALT level. *C,* Correlation between heat shock protein 70 (HSP70) level and HBV DNA level. *D,* Correlation between HSP70 level and ALT level.
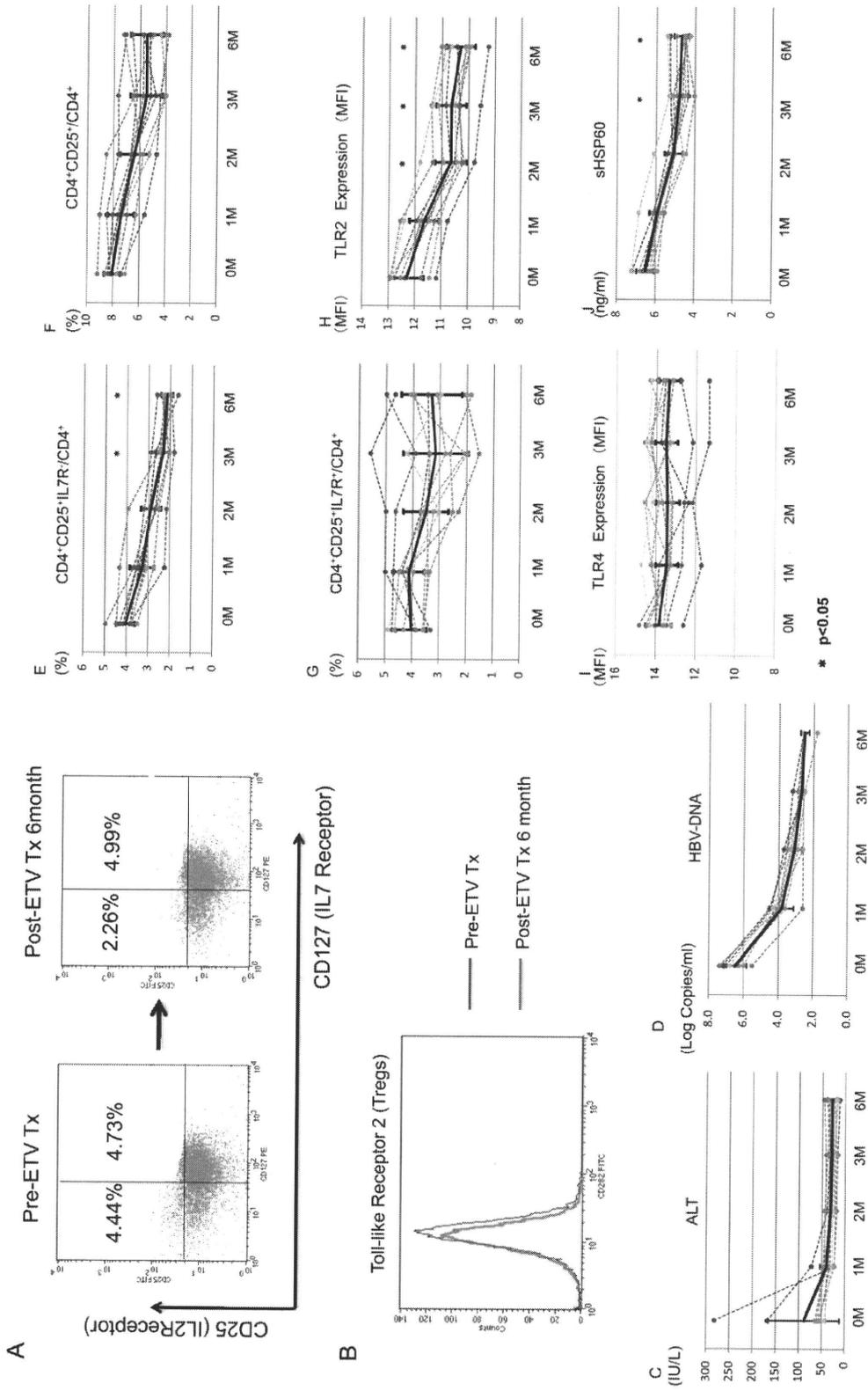
Figure 7. Sequential analysis of primary lymphocytes and soluble heat shock protein 60 (sHSP60) during entecavir (ETV) therapy. *A,* Representative dot plots of the CD4⁺CD25⁺IL7R⁻ cells before treatment and 6 months after the start of treatment. Peripheral blood mononuclear cells were stained with anti-CD3, anti-CD4, anti-CD25, and anti-IL7R (CD127). The phenotypes of the CD4⁺ cells were determined as follows: CD4⁺CD25⁺IL7R⁻ cells were identified as regulatory cells and CD4⁺CD25⁺IL7R⁺ cells were identified as activated CD4⁺ cells. *B,* Representative histogram of Toll-like receptor 2 (TLR2) surface expression on CD4⁺CD25⁺ regulatory T (T_reg) cells before treatment and 6 months after the start of treatment. *C* and *D,* Serum levels of alanine aminotransferase (ALT) and hepatitis B virus (HBV) DNA during ETV treatment. Solid black lines and error bars indicate the mean values and standard deviations, respectively. *E–G,* Frequencies of CD4⁺CD25⁺IL7R⁻ cells, CD4⁺CD25⁺ cells, and CD4⁺CD25⁺IL7R⁺ cells among CD4⁺ cells during ETV treatment. *H* and *I,* Mean fluorescence intensity (MFI) of TLR2 and Toll-like receptor 4 (TLR4) expression on CD4⁺CD25⁺ cells during ETV treatment. *J,* Serum levels of sHSP60 during ETV treatment. *P <.01 for comparison between pretreatment levels and posttreatment levels.

Figure 8. Frequency of CD4+CD25+FoxP3+ cells.

CD4+CD25+FoxP3+ cells was also decreased during lamivudine therapy. Moreover, the expression level of TLR2 on CD4+CD25+ cells gradually declined during entecavir therapy (Figure 7G).

Suppressive activity of T$_{reg}$ cells. The suppressive activity of T$_{reg}$ cells was analyzed by means of coincubation of unstained isolated T$_{reg}$ cells and autologous CD4+CD25− cells with CFSE staining. Ex vivo peripheral blood samples from 10 selected patients were analyzed before treatment, 3 months after the start of treatment, and 6 months after the start of treatment. The mean fluorescence intensity of the CFSE staining of the CD4+CD25− cells was statistically significantly decreased at 6 months after the start of treatment ($P < .05$). These data indicate that the suppressive activity of T$_{reg}$ cells was gradually decreased during entecavir treatment.

DISCUSSION

In this study, we have demonstrated that the levels of sHSP60 in patients with chronic hepatitis B were statistically significantly higher than those in patients with chronic hepatitis C. Moreover, the levels of sHSP60 were correlated with the HBV DNA levels but not with the ALT levels. On the other hand, the levels of sHSP70 were correlated with the ALT levels but not with the HBV DNA levels. This discrepancy in the correlation might be due to differences in the mechanism of heat shock protein production or secretion. The release of such heat shock proteins from cells is triggered by physical trauma and behavioral stress as well as by exposure to immunological danger signals [31, 32]. Stress protein release occurs both through physiological secretion mechanisms and during cell death by necrosis [33, 34]. HSP60 might be induced by the stress of HBV replication, because the levels of HSP60 were clearly correlated with the HBV DNA levels. On the other hand, HSP70 secretion might also be caused by cell death, because the levels of sHSP70 were correlated with the ALT levels. However, we should wait for more detailed studies about the HBV-specific induction of HSP60 to confirm this correlation. Extracellular stress proteins of the heat shock protein and glucose-regulated stress protein families, including HSP60, have powerful effects on the immune response [35]. Moreover, various kinds of immune cells such as macrophages, dendritic cells, CD4+effector T cells, and T$_{reg}$ cells are affected by heat shock proteins [28, 35]. Most recently, Cohen-Sfady et al [36] reported that HSP60 enhanced the activity of IL-10 secretion from B cells. This effect could support our findings of the immune-suppressive effect of HSP60. However, we can not draw conclusions about the whole effects of immune responses because the various kinds of immune cells might affect each other by means of cytokines, chemokines, stress-related proteins, and direct binding.

In this study, we focused on the effect of HSP60 on T$_{reg}$ cell function by isolating T$_{reg}$ cells, because many research groups had reported that the function and frequency of T$_{reg}$ cells might be related to HBV replication. T$_{reg}$ cells play an important role in the immune-hyporesponsiveness of patients with chronic hepatitis B. Previously, we demonstrated that the polarization of CD4+ T cells was suppressed when the cells were stimulated with HBcAg in patients with chronic hepatitis B. T$_{reg}$ cells are important cells in the suppression of the T helper 1 cell response by HBcAg, as demonstrated by the increased population of IL-10-secreting CD4+CD25+ cells. This indicates the presence of an inducible T$_{reg}$ cell population, which is specific for HBcAg and produces IL-10, as well as a natural T$_{reg}$ cell population in patients with chronic hepatitis B. Pretreatment with rHSP60 increased the frequency of HBcAg-specific IL-10-secreting CD4+CD25+ cells and enhanced the IL-10-secreting activity. These results indicate that pretreatment with rHSP60 might enhance the susceptibility of the HBcAg response and the function of IL-10 production by T$_{reg}$ cells. These data might not imply that there was an expansion of HBcAg-specific T$_{reg}$ cells as a result of the rHSP60 pretreatment, because the incubation phase was for only 16 h (4 h of pretreatment with rHSP60 plus 12 h of coincubation with HBcAg-presenting APCs). However, there is a possibility that continuous exposure to sHSP60 might induce an expansion of T$_{reg}$ cells by enhancing the sensitivity of the expansion signal.

In this study, we found that the effect of HSP60 could be blocked by TLR2 neutralizing antibody but not by TLR4 neutralizing antibody. These data indicate that the effect of HSP60 could depend on TLR2. During entecavir therapy, not only the frequency of T$_{reg}$ cells but also the serum levels of HSP60 and surface expression of TLR2 on T$_{reg}$ cells gradually decreased. Therefore, we performed the suppression assay to detect the activity of T$_{reg}$ cells by use of ex vivo isolated T$_{reg}$ cells. The results of this suppression assay indicate that the reduction of the HBV DNA level could suppress the excessive activity of T$_{reg}$ cells. In our previous study, the frequency and the function of HBV-specific cytotoxic T lymphocytes were partially recovered after therapy with nucleoside or nucleotide analogues [11]. The results clearly indicate that this restoration might be due to not only the reduction of HBV antigens but also the reduction of the frequency and function of T$_{reg}$ cells.

On the basis of genomic analysis, 8 genotypes (A–H) of HBV have been defined, among which genotypes A, B, and especially C are prevalent in Japan [37–40]. Previous studies suggested that the clinical outcome of chronic hepatitis B was more severe in patients infected with genotype C, compared with those infected with genotype B [38, 39]. In this study, most of the

samples had HBV genotype C because of the high frequency of HBV genotype C infection in Japan. However, the expression levels of HSP60 were different among samples with the various genotypes in preliminary in vitro studies (data not shown). In addition, the expression patterns of chemokines in HBV-replicating Huh7 cells are apparently different among the various genotypes (Y. Kondo et al, unpublished data, May 2009). However, during entecavir treatment, the level of sHSP60 production in patients with genotype Bj HBV infection was quite similar to that in patients with genotype C HBV infection. We could not determine the relevance of the HBV genotypes and sHSP60 production levels because of the small numbers of genotype Bj–infected patients in this study.

In conclusion, we found that HSP60 was produced by HBV-replicating hepatocytes and determined the relevance of sHSP60 to T_{reg} cells functions, especially for IL-10-secreting activity. The understanding of the immunopathogensis of chronic hepatitis B could contribute to the development of novel kinds of immune therapy. Combination therapy with nucleoside or nucleotide analogues should be a reasonable method, because the suppression of HBV replication could reduce the excessive immune tolerance induced by T_{reg} cells.

References

1. Tiollais P, Pourcel C, Dejean A. The hepatitis B virus. Nature 1985; 317:489–495.
2. Lai CL, Ratziu V, Yuen MF, Poynard T. Viral hepatitis B. Lancet 2003; 362:2089–2094.
3. Kagi D, Ledermann B, Burki K, Zinkernagel RM, Hengartner H. Molecular mechanisms of lymphocyte-mediated cytotoxicity and their role in immunological protection and pathogenesis in vivo. Annu Rev Immunol 1996; 14:207–232.
4. Peng G, Li S, Wu W, Sun Z, Chen Y, Chen Z. Circulating CD4+ CD25+ regulatory T cells correlate with chronic hepatitis B infection. Immunology 2008; 123:57–65.
5. Barboza L, Salmen S, Goncalves L, et al. Antigen-induced regulatory T cells in HBV chronically infected patients. Virology 2007; 368:41–49.
6. Kondo Y, Ueno Y, Shimosegawa T. Immunopathogenesis of hepatitis B persistent infection: implications for immunotherapeutic strategies. Clin J Gastroenterol 2009; 2:71–79.
7. Xu D, Fu J, Jin L, et al. Circulating and liver resident CD4+CD25+ regulatory T cells actively influence the antiviral immune response and disease progression in patients with hepatitis B. J Immunol 2006; 177: 739–747.
8. Manigold T, Racanelli V. T-cell regulation by CD4 regulatory T cells during hepatitis B and C virus infections: facts and controversies. Lancet Infect Dis 2007; 7:804–813.
9. Kondo Y, Kobayashi K, Ueno Y, et al. Mechanism of T cell hyporesponsiveness to HBcAg is associated with regulatory T cells in chronic hepatitis B. World J Gastroenterol 2006; 12:4310–4317.
10. Kondo Y, Kobayashi K, Asabe S, et al. Vigorous response of cytotoxic T lymphocytes associated with systemic activation of CD8 T lymphocytes in fulminant hepatitis B. Liver Int 2004; 24:561–567.
11. Kondo Y, Asabe S, Kobayashi K, et al. Recovery of functional cytotoxic T lymphocytes during lamivudine therapy by acquiring multi-specificity. J Med Virol 2004; 74:425–433.
12. Chisari FV, Ferrari C. Hepatitis B virus immunopathogenesis. Annu Rev Immunol 1995; 13:29–60.
13. Reignat S, Webster GJ, Brown D, et al. Escaping high viral load exhaustion: CD8 cells with altered tetramer binding in chronic hepatitis B virus infection. J Exp Med 2002; 195:1089–1101.
14. Suri-Payer E, Amar AZ, Thornton AM, Shevach EM. CD4+CD25+ T cells inhibit both the induction and effector function of autoreactive T cells and represent a unique lineage of immunoregulatory cells. J Immunol 1998; 160:1212–1218.
15. Chen W, Jin W, Hardegen N, et al. Conversion of peripheral CD4+CD25− naive T cells to CD4+CD25+ regulatory T cells by TGF-beta induction of transcription factor Foxp3. J Exp Med 2003; 198:1875–1886.
16. Hori S, Nomura T, Sakaguchi S. Control of regulatory T cell development by the transcription factor Foxp3. Science 2003; 299:1057–1061.
17. Suvas S, Kumaraguru U, Pack CD, Lee S, Rouse BT. CD4+CD25+ T cells regulate virus-specific primary and memory CD8+ T cell responses. J Exp Med 2003; 198:889–901.
18. Nakamura K, Kitani A, Fuss I, et al. TGF-beta 1 plays an important role in the mechanism of CD4+CD25+ regulatory T cell activity in both humans and mice. J Immunol 2004; 172:834–842.
19. Zheng SG, Wang JH, Gray JD, Soucier H, Horwitz DA. Natural and induced CD4+CD25+ cells educate CD4+CD25− cells to develop suppressive activity: the role of IL-2, TGF-beta, and IL-10. J Immunol 2004; 172:5213–5221.
20. Sundstedt A, O'Neill EJ, Nicolson KS, Wraith DC. Role for IL-10 in suppression mediated by peptide-induced regulatory T cells in vivo. J Immunol 2003; 170:1240–1248.
21. Ulsenheimer A, Gerlach JT, Gruener NH, et al. Detection of functionally altered hepatitis C virus-specific CD4 T cells in acute and chronic hepatitis C. Hepatology 2003; 37:1189–1198.
22. Marshall NA, Vickers MA, Barker RN. Regulatory T cells secreting IL-10 dominate the immune response to EBV latent membrane protein 1. J Immunol 2003; 170:6183–6189.
23. Beilharz MW, Sammels LM, Paun A, et al. Timed ablation of regulatory CD4+ T cells can prevent murine AIDS progression. J Immunol 2004; 172:4917–4925.
24. Wallin RP, Lundqvist A, More SH, von Bonin A, Kiessling R, Ljunggren HG. Heat-shock proteins as activators of the innate immune system. Trends Immunol 2002; 23:130–135.
25. Raz I, Elias D, Avron A, Tamir M, Metzger M, Cohen IR. Beta-cell function in new-onset type 1 diabetes and immunomodulation with a heat-shock protein peptide (DiaPep277): a randomised, double-blind, phase II trial. Lancet 2001; 358:1749–1753.
26. Hu W, Hasan A, Wilson A, et al. Experimental mucosal induction of uveitis with the 60-kDa heat shock protein-derived peptide 336–351. Eur J Immunol 1998; 28:2444–2455.
27. Mor F, Cohen IR. T cells in the lesion of experimental autoimmune encephalomyelitis: enrichment for reactivities to myelin basic protein and to heat shock proteins. J Clin Invest 1992; 90:2447–2455.
28. Zanin-Zhorov A, Cahalon L, Tal G, Margalit R, Lider O, Cohen IR. Heat shock protein 60 enhances CD4+ CD25+ regulatory T cell function via innate TLR2 signaling. J Clin Invest 2006; 116:2022–2032.
29. Sugiyama M, Tanaka Y, Kato T, et al. Influence of hepatitis B virus genotypes on the intra- and extracellular expression of viral DNA and antigens. Hepatology 2006; 44:915–924.
30. Inoue J, Takahashi M, Nishizawa T, et al. High prevalence of hepatitis delta virus infection detectable by enzyme immunoassay among apparently healthy individuals in Mongolia. J Med Virol 2005; 76:333–340.
31. Lindquist S, Craig EA. The heat-shock proteins. Annu Rev Genet 1988; 22:631–677.
32. Ellis RJ. The molecular chaperone concept. Semin Cell Biol 1990; 1: 1–9.
33. Hightower LE, Guidon PT Jr. Selective release from cultured mammalian cells of heat-shock (stress) proteins that resemble glia-axon transfer proteins. J Cell Physiol 1989; 138:257–266.
34. Mambula SS, Calderwood SK. Heat shock protein 70 is secreted from

tumor cells by a nonclassical pathway involving lysosomal endosomes. J Immunol **2006**; 177:7849–7857.

35. Calderwood SK, Mambula SS, Gray PJ Jr, Theriault JR. Extracellular heat shock proteins in cell signaling. FEBS Lett **2007**; 581:3689–3694.

36. Cohen-Sfady M, Pevsner-Fischer M, Margalit R, Cohen IR. Heat shock protein 60, via MyD88 innate signaling, protects B cells from apoptosis, spontaneous and induced. J Immunol **2009**; 183:890–896.

37. Mahmood S, Niiyama G, Kamei A, et al. Influence of viral load and genotype in the progression of hepatitis B-associated liver cirrhosis to hepatocellular carcinoma. Liver Int **2005**; 25:220–225.

38. Akuta N, Suzuki F, Kobayashi M, et al. Virological and biochemical relapse after discontinuation of lamivudine monotherapy for chronic hepatitis B in Japan: comparison with breakthrough hepatitis during long-term treatment. Intervirology **2005**; 48:174–182.

39. Kobayashi M, Suzuki F, Akuta N, et al. Response to long-term lamivudine treatment in patients infected with hepatitis B virus genotypes A, B, and C. J Med Virol **2006**; 78:1276–1283.

40. Tanaka Y, Mizokami M. Genetic diversity of hepatitis B virus as an important factor associated with differences in clinical outcomes. J Infect Dis **2007**; 195:1–4.

Differential transcriptional characteristics of small and large biliary epithelial cells derived from small and large bile ducts

S. Glaser,[1,2]* M. Wang,[3]* Y. Ueno,[4] J. Venter,[5] K. Wang,[3] H. Chen,[3] G. Alpini,[1,2,5] and A. Holterman[3]

[1]Scott and White Digestive Disease Research Center, and [2]Central Texas Veterans Health Care System, Temple, Texas; [3]Departments of Pediatrics and Surgery, RUSH University Medical Center, Chicago, Illinois; [4]Tohoku University Graduate School of Medicine, Miyagi, Japan; and [5]Division of Gastroenterology, Department of Medicine, College of Medicine, Texas A&M Health Science Center, College Station, Texas

Glaser S, Wang M, Ueno Y, Venter J, Wang K, Chen H, Alpini G, Holterman A. Differential transcriptional characteristics of small and large biliary epithelial cells derived from small and large bile ducts. Am J Physiol Gastrointest Liver Physiol 299: G769–G777, 2010. First published June 24, 2010; doi:10.1152/ajpgi.00237.2010.— Biliary epithelial cells (BEC) are morphologically and functionally heterogeneous. To investigate the molecular mechanism for their diversities, we test the hypothesis that large and small BEC have disparity in their target gene response to their transcriptional regulator, the biliary cell-enriched hepatocyte nuclear factor HNF6. The expression of the major HNF (*HNF6, OC2, HNF1b, HNF1a, HNF4a, C/EBPb,* and *Foxa2*) and representative biliary transport target genes that are HNF dependent were compared between SV40-transformed BEC derived from large (SV40LG) and small (SV40SM) ducts, before and after treatment with recombinant adenoviral vectors expressing *HNF6* (AdHNF6) or control *LacZ* cDNA (AdLacZ). Large and small BEC were isolated from mouse liver treated with growth hormone, a known transcriptional activator of HNF6, and the effects on selected target genes were examined. Constitutive *Foxa2, HNF1a,* and *HNF4a* gene expression were 2.3-, 12.4-, and 2.6-fold, respectively, higher in SV40SM cells. This was associated with 2.7- and 4-fold higher baseline expression of HNF1a- and HNF4a-regulated *ntcp* and *oatp1* genes, respectively. Following AdHNF6 infection, *HNF6* gene expression was 1.4-fold higher (*P* = 0.02) in AdHNF6 SV40SM relative to AdHNF6 SV40LG cells, with a corresponding higher *Foxa2* (4-fold), *HNF1a* (15-fold), and *HNF4a* (6-fold) gene expression in AdHNF6-SV40SM over AdHNF6-SV40LG. The net effects were upregulation of HNF6 target gene *glucokinase* and of Foxa2, HNF1a, and HNF4a target genes *oatp1, ntcp,* and *mrp2* over AdLacZ control in both cells, but with higher levels in AdH6-SV40SM over AdH6-SV40LG of *glucokinase, oatp1, ntcp,* and *mrp2* (by 1.8-, 3.4-, 2.4-, and 2.5-fold, respectively). In vivo, growth hormone-mediated increase in *HNF6* expression was associated with similar higher upregulation of *glucokinase* and *mrp2* in cholangiocytes from small vs. large BEC. Small and large BEC have a distinct profile of hepatocyte transcription factor and cognate target gene expression, as well as differential strength of response to transcriptional regulation, thus providing a potential molecular basis for their divergent function.

heterogeneity; bile transport; hepatocyte nuclear factors; hepatocyte nuclear factor 6

HEPATIC GENE EXPRESSION IS primarily regulated at the transcriptional level by families of hepatocyte nuclear factors (HNF). Among these, the homeodomain HNF1, the orphan nuclear receptor HNF4, the ONECUT HNF6 (also known as OC-1 and OC-2), forkhead box (FoxA), and the CCATT/enhancer-binding proteins (C/EBP) are cell-autonomous, liver-enriched transcription factors bearing specific DNA-binding domains, which recognize cognate DNA motifs on the regulatory region of hepatic target genes to participate in a cross-regulatory network for modulating target gene activities (10, 36). In vivo, HNF participate in the liver developmental program. For instance, Foxa1 and Foxa2 are implicated in hepatic specification (24), HNF4a in hepatic fate determination (30), and OC1 and OC2 in biliary cell lineage specification (8). HNF also participate in the regulation of hepatic function in the mature liver, including glucose metabolism by HNF4a (39), HNF1a (25), HNF6 (22), or cholesterol and bile acid metabolism by HNF6 (41) and Foxa2 (7).

The liver is the largest internal organ of the body and is composed of two types of epithelial cells: *1*) hepatocytes and *2*) cholangiocytes (2). Hepatocytes account for ~70% and cholangiocytes for 3–5% of the endogenous liver cell population. Cholangiocytes [also known as biliary epithelial cells (BEC)] populate the bile ducts (2). The intrahepatic bile duct size ranges from large ducts emanating from the confluence of the extrahepatic bile ducts at the liver hilum to progressively smaller intrahepatic ducts (19). In experimental models, small BEC refer to BEC lining the small bile ducts, whereas large BEC line larger biliary ducts (3, 15). Small and large rodent BEC have distinct morphometry (15), gene expression profile (38), as well as proliferative, apoptotic, and secretory responses to experimental stimuli (1, 14, 15). This BEC heterogeneity is clinically relevant in that the large and small ducts are differentially targeted in human cholangiopathies (37), stressing the importance of understanding the molecular mechanism regulating their functional diversities.

Since hepatocytes and BEC embryonic cellular origins are from multipotent hepatoblasts (34), it is not surprising that they have overlapping physiological function, such as solute secretion and metabolic activities (23), and are, therefore, likely to share transcriptional regulation. Compared with BEC, the role of HNF in the molecular regulation of differentiated liver-specific genes in hepatocytes is better understood (10, 36). Among HNFs, the current body of data suggest that HNF6 is a dominant BEC-enriched transcription factor. It is critical to the early commitment of hepatoblasts to the biliary epithelial lineage as mutant mice with global HNF6 deletion exhibit biliary duct malformations and early mortality from cholestasis (9). Our laboratory has shown that HNF6 transcription factor is also highly expressed in BEC in the mature mouse liver and can negatively regulate BEC proliferation during early bile

duct ligation injury (17). The transcriptional regulation of hepatic target genes by HNF6 is broad, involving gene with metabolic and transport function (22, 29, 35, 41), as well as other HNF, such as *HNF4a* (21), *HNF1b* (9), and *Foxa2* (21), suggesting that HNF6 can comprehensively regulate the biliary cell molecular signature, and that enforced HNF6 expression in large and small biliary cells would elucidate the molecular basis for their heterogeneity. To further our understanding of BEC gene regulation, we herein test the hypothesis that the biliary cell-enriched transcription factor HNF6 differentially regulates the large and small BEC downstream transcriptional events. We first characterized the expression profile of HNF and selected HNF target genes in the SV40 large T antigen-transformed and immortalized large and small BEC (SV40LG and SV40SM, respectively). We compared changes in the BEC transcriptional response to increasing HNF6 expression in these cell lines using recombinant adenoviral vectors expressing *HNF6* cDNA (AdHNF6). We evaluated representative in vivo HNF6 target gene expression in large and small BEC isolated from liver tissues following administration of HNF6-enhancing vector growth hormone (GH), a known STAT5-mediated transcriptional activator of HNF6 promoter (21).

MATERIALS AND METHODS

Materials. SV40LG and SV40SM BEC were derived from BALB/c mice and characterized as previously described (38). The construction and preparation of the replication-defective recombinant adenoviral vectors expression of the bacterial LacZ (AdLacZ) or mouse HNF6 cDNA (AdHNF6) have been reported (41). HNF6, HNF1a, HNF4a, Foxa2, C/EBPb, and β-actin antibodies were obtained from Santa Cruz Technology.

Cell culture. As previously described (15), cells were incubated at 37°C in 5% CO_2 atmosphere in D-MEM (Gibco) supplemented with 10% FBS, 1% pen/strep, and 1% L-glutamine. For experiments (n = 4), cells were plated at 5×10^6 cells in 10-cm culture dishes for mock infection or infection with a multiplicity of infection of 35 infectious units of AdHNF6 or AdLacZ in 1 ml of media for 60 min, following which media was added to a final 10-ml volume. Cells were harvested after 24 h of infection and washed three times with PBS to remove residual virus for subsequent total RNA extraction.

Animal procedures. Six- to eight-week-old male CD1 mice were kept in a 12:12-h light-dark-cycles with free access to standard chow and water. All animals received humane care, according to the criteria outlined in the Guide for the Care and Use of Laboratory Animals by the National Academy of Sciences and the National Institutes of Health (NIH). The animal care and use section of the NIH funding application was reviewed in accordance with the policies of the Institutional Animal Care and Use Committee and approved. Mice received an initial intraperitoneal injection of human recombinant GH (obtained from the National Institute of Diabetes and Digestive and Kidney Diseases National Hormone and Peptide Program) at 4 μg/g body wt, followed by a 3 μg/g body wt injection every 6 h and killed after 24 h for BEC isolation and purification.

BEC isolation. The procedure was described previously (2) but briefly, following in situ collagenase perfusion, in three different experiments, the cholangiocyte mixture from the biliary tracts were separated into large and small cells by counterflow elutriation (3) with further purification by immunoaffinity using immunomagnetic beads. Glucose-6-phosphatase and vimentin immunostaining was done to rule out contamination by hepatocytes and mesenchymal cells, respectively (1).

Gene analyses. Total liver RNA was extracted using RNA-STAT-60 (Tel-Test "B", Friendswood, TX). Following DNase I (Ambion, Austin, TX) digestion, cDNA was synthesized using the cDNA Synthesis Kit (Biorad, Hercules, CA) and purified through Qiagen column. Reactions were amplified using the appropriate primer sets and analyzed in triplicate using a MyiQ Single Color Real-Time PCR Detection System (Biorad). The relative expression of the genes was calculated by a mathematical delta-delta method developed by PE Applied Biosystems. Levels were reported after normalization to housekeeping gene cyclophilin for each gene. The primers sequences for mouse genes are provided in Table 1.

Western blot assays. Crude protein extracts were prepared from AdHNF-6 infected SV40LG and SV40SM cells, and protein concentrations were determined using the Bradford method (Bio-Rad). HNF6, HNF1a, HNF4a, Foxa2, C/EBPb, and β-actin immune complexes were detected with horseradish-conjugated secondary antibody (Fisher), followed by chemiluminescence (ECL + plus, Amersham Biosciences).

Statistical analysis. All data are expressed as means ± SD, unless otherwise indicated. Intergroup differences were evaluated by analysis of variance for repeated measures. A P value of <0.05 is considered to be significant. All statistical analyses were performed with the software SPSS.

RESULTS

Constitutive expression of hepatocyte transcription factors in SV40LG and SV40SM cells. The SV40 large T antigen-transformed large (SV40LG) and small BEC (SV40SM), derived from large and small bile ducts of mouse liver, were

Table 1. *Primer sequences for mouse genes*

Gene	Primers	
	Forward sequence	Reverse sequence
Transcription factors		
HNF1a	5'-TTC TAA GCT GAG CCA GCT GCA GAC G-3'	5'-GCT GAG GTT CTC CGG CTC TTT CAG A-3'
HNF1b	5'-GAA AGC AAC GGG AGA TCC TC-3'	5'-CCT CCA CTA AGG CCT CCC TC-3'
HNF6	5'-GGT CTG GGC AGC ATT CAC AAC-3'	5'-CAG GGT GGT GGG CTT CAA AG-3'
HNF4a	5'-ACA CGT CCC CAT CTG AAG-3'	5'-CTT CCT TCT TCA TGC CAG-3'
C/EBPb	5'-ATC GAC TTC AGC CCC TAC CT-3'	5'-GGC TCA CGT AAC CGT AGT CG-3'
Foxa2	5'-CCA TCA GCC CCA CAA AAT G-3'	5'-CCA AGC TGC CTG GCA TG-3'
Hepatic function genes		
Glucokinase	5'-CCT GGG CTT CAC CTT CTC CTT-3'	5'-GAG GCC TTG AAG CCC TTG GT-3'
Mrp2	5'-AGA GGG CGG TGA CAA CCT GAG-3'	5'-CCG ATG GTC GTC TGA ATG AGG-3'
Ntcp	5'-ATG ACC ACC TGC TCC AGC TT-3'	5'-GCC TTT GTA GGG CAC CTT GT-3'
Oatp1	5'-AAT TTG GGA AGA GTG GCC TT	5'-TGG AGT CAA TGC AAA AAC CA
TGFb2R	5'-CGG AAA TTC CCA GCT TCT GG-3'	5'-TTT GGT AGT GTT CAG CGA GC-3'

Sequences are annotated with the binding position upstream of the transcription start site. See text for definitions of gene acronyms.

previously characterized (38) and shown to display morphological, phenotypic, and functional characteristics of freshly isolated large and small cholangiocytes (15). The baseline profile in the expression of hepatocyte transcription factors *HNF6* (*OC1*) and its paralog *OC2* (18), *HNF1b*, *HNF1a*, *HNF4a*, *Foxa2*, and *C/EBPb* was assessed by real-time PCR in SV40LG and SV40SM cell lines. Figure 1 illustrates that, while *HNF6*, *OC2*, *HNF1b*, and *C/EBPb* gene expression levels were comparable in small and large BEC, *Foxa2*, *HNF1a*, and *HNF4a* levels were 2.3-fold ($P = 0.001$), 12.4-fold ($P = 0.001$), and 2.6-fold ($P = 0.02$), respectively, higher in SV40SM cells. Consistent with the fact that HNF expression is primarily regulated at the transcriptional level, Western blotting for protein expression (Fig. 1*B*) exhibits the same pattern of higher *Foxa2*, *HNF1a*, and *HNF4a* levels in SV40SM cells.

Constitutive expression of HNF target genes in SV40LG and SV40SM cells. Intrahepatic bile acid transport is among many of BEC important functions (26). We next examined the expression of hepatic bile acid transport genes, which are known target genes for HNF: *ntcp* (the Na$^+$-dependent taurocholate cotransport peptide for bile acid import, also known as slc10a1) is transcriptionally regulated by *HNF1a* (13) and *HNF4a* (13, 16); *mrp2* (the multidrug resistance-associated protein for xeno- and endobiotics bile acid export, also known as abcc2) by *HNF1a* and *HNF4a* (20, 32), and possibly by *Foxa2* (7); and *oatp1* (the organic anion transporter for basolateral bile acid uptake, also known as slc21a1) by *HNF1a* (4, 27) and *HNF4a* (11, 16). Since the above data showed that SV40LG and SV40SM cells have differential expression of *Foxa2*, *HNF1a*, and *HNF4a* transcription factors, we next sought to characterize the baseline expression of *HNF6*, *Foxa2*, *HNF1a*, and *HNF4a* target genes. As control target genes for *HNF6*, we assayed *glucokinase (GK*, previously shown to be positively regulated by HNF6) (22) and *TGFb2R* (shown to be negatively regulated by HNF6) (31, 40) and did not find differences in their baseline expression (Fig. 2). HNF1a/HNF4a target genes *ntcp* and *oatp1* are expressed at 2.7-fold ($P = 0.004$) and 4-fold higher levels ($P = 0.01$) in SV40SM than SV40LG cells. Since *mrp2* expression levels were low, the biological significance of a statistical difference in the expression between SV40LG and SV40SM cells (1.6-fold higher in SV40SM, $P = 0.001$) is not clear.

Effects of increasing HNF6 expression in BEC on known HNF6 target genes. Since HNF6 is a major BEC-enriched transcription factor, cells were mock infected or treated with AdLacZ and AdHNF6 to assess if increasing HNF6 expression can transcriptionally alter BEC gene profiles. Since mock-infected cells have comparable gene expression levels as AdLacZ-infected cells (data not shown), the results comparing AdLacZ- against AdHNF6-infected cells are presented (Table 2). Previous studies have shown that AdHNF6 tail vein injection effectively increased *HNF6* gene and nuclear protein expression in both hepatocytes and bile ducts (17). Following AdHNF6 treatment, *HNF6* gene expression was also appropriately increased in AdHNF6-SV40LG and AdHNF6-SV40SM cells relative to AdLacZ-treated control by 1,450-fold and 2,608-fold, respectively, corresponding to a 1.4-fold higher HNF6 expression in AdHNF6-SV40SM relative to AdHNF6-SV40LG ($P = 0.02$) (Table 1). Western blotting of AdLacZ- and AdHNF6-infected SV40LG and SV40SM cells confirmed a similar pattern of higher HNF6 protein expression in AdHNF6-SV40SM cells (Fig. 3). HNF6 target gene *TGFb2R* (Table 2) changed minimally in AdHNF6-infected SV40LG, but, con-
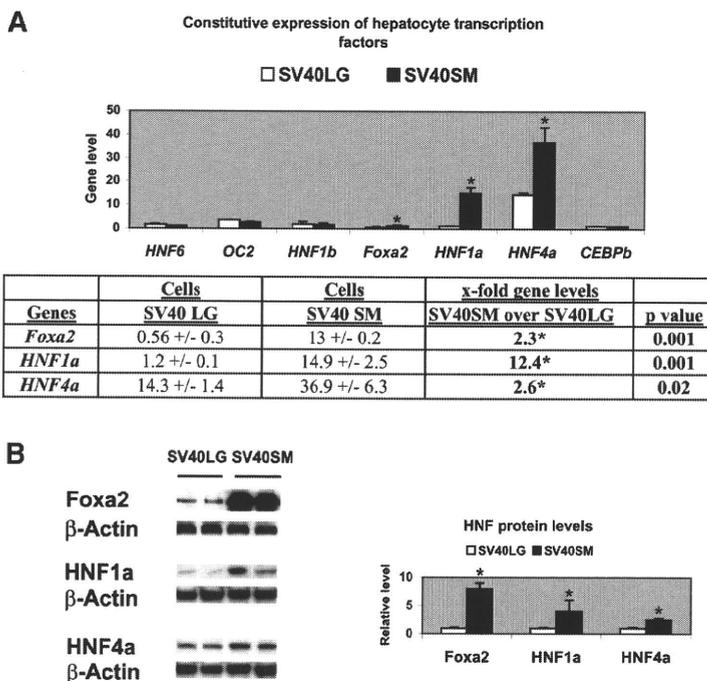

A Constitutive expression of hepatocyte transcription factors

☐ SV40LG ■ SV40SM

Genes	Cells	Cells	x-fold gene levels	
	SV40 LG	**SV40 SM**	**SV40SM over SV40LG**	**p value**
Foxa2	0.56 +/- 0.3	13 +/- 0.2	2.3*	0.001
HNF1a	1.2 +/- 0.1	14.9 +/- 2.5	12.4*	0.001
HNF4a	14.3 +/- 1.4	36.9 +/- 6.3	2.6*	0.02

B SV40LG SV40SM

Foxa2
β-Actin

HNF1a
β-Actin

HNF4a
β-Actin

HNF protein levels
☐SV40LG ■SV40SM

Fig. 1. Constitutive expression of hepatocyte transcription factors in SV40LG (large) and SV40SM (small) cell lines. *A*: real-time PCR bar graph of *HNF6*, *OC2*, *HNF1a*, *HNF1b*, *Foxa2*, *HNF4a*, and *C/EBPb* gene levels (after normalization to housekeeping gene *cyclophilin*), showing higher *Foxa2*, *HNF1a*, and *HNF4a* in SV40SM over SV40LG cells. The table shows *Foxa2*, *HNF1a*, and *HNf4a* gene levels and the x-fold higher expression with the corresponding *P* values in SV40SM over SV40LG cells. *B*: Western blotting micrographs of Foxa2, HNF1a, HNF4a, and β-actin protein expression in SV40LG and SV40SM cells. Bar graph of densitometry analysis of the immune complexes after normalization with β-actin shows higher Foxa2, HNF1a, and HNF4a expression levels in SV40SM cells relative to SV40LG cells. *P values of significance at <0.05. See text for definitions of gene acronyms used in figures.
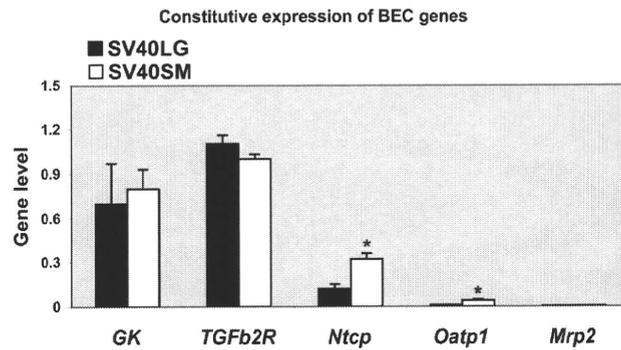
- 371 -

Fig. 2. Constitutive expression of target genes in SV40LG and SV40SM cell lines. Real-time PCR bar graph shows *glucokinase* (*GK*), *TGFb2R*, *ntcp*, *oatp1*, and *mrp2* gene levels, and table shows *ntcp*, *oatp1a1*, and *mrp2* gene levels and the x-fold higher expression in SV40SM over SV40LG cells with the corresponding *P* values. *Significant *P* values.

Genes	Cells SV40 LG	Cells SV40 SM	x-fold gene levels SV40SM over SV40LG	p value
GK	0.7 +/- 0.27	0.8 +/- 0.13	1.1	0.5
TGFb2R	1.1 +/- 0.06	1 +/- 0.03	1	0.7
Ntcp	0.12 +/- 0.03	0.32 +/- 0.04	2.7*	0.004
Oatp1	0.01 +/- 0.001	0.04 +/- 0.01	4*	0.01
Mrp2	0.001 +/- 0.001	0.0016 +/- 0.001	(1.6)	(0.001)

sistent with the higher expression of *HNF6* in AdHNF6-SV40SM cells, its level is 1.6-fold more diminished in AdHNF6-SV40SM relative to AdHNF6-SV40LG cells (*P* = 0.03). HNF6 target gene *glucokinase* response was more dramatic, with a 16- and 38-fold upregulation following AdHNF6 infection over AdLacZ control in AdHNF6-SV40LG and AdHNF6-SV40SM cells, respectively, corresponding to an 1.8-fold higher (*P* = 0.02) *glucokinase* expression in AdHNF6-SV40SM cells compared with AdHNF6-SV40LG cells. These results demonstrate that BEC and hepatocytes display similar HNF6 target gene response, but most of all, that small BEC have higher reactivity to HNF6 transcriptional regulation.

Effects of increasing HNF6 BEC expression on other HNF and HNF-regulated bile transport target genes. We next evaluated the effect of HNF6 overexpression on the transcriptional response of other known HNF6-dependent HNF [such as *HNF4a* (21), *HNF1b* (9), and *Foxa2* (21)] in BEC (Fig. 4). Despite an unexpected AdHNF6-associated suppression of endogenous HNF4a gene levels (Fig. 4*B*) in both SV40SM (by 2-fold, *P* = 0.05) and SV40LG cells (by 6.4-fold, *P* = 0.002), the net effect of higher *HNF6* expres-

sion in AdHNF6-SV40SM over AdHNF6-SV40LG BEC is illustrated in Fig. 4*A*, demonstrating that the final *Foxa2*, *HNF1a*, and *HNF4a* expression in AdHNF6-infected small BEC remained markedly higher than in AdHNF6-infected large BEC, with a 4-fold (*P* = 0.01), 15-fold (*P* = 0.001), and 6.5-fold (*P* = 0.03) difference, respectively.

Effects of AdHNF6 treatment on HNF-regulated bile transport target genes. As seen in Fig. 5, the response to AdHNF6 infection in both SV40LG and SV40SM cells of the biliary genes was characterized in AdHNF6-SV40 cells relative to AdLacZ-SV40 cells by upregulation of *ntcp*, *oatp1*, and *mrp2* expression with enhanced *ntcp* (5.3-fold up, *P* = 0.001, Fig. 5*A*), *oatp1* (5-fold up, *P* = 0.001, Fig. 5*B*), and *mrp2* (24-fold up, *P* = 0.01, Fig. 5*C*) expression in AdHNF6-SV40 LG cells, and increased *ntcp* by 6.5-fold (*P* = 0.001, Fig. 5*A*), *oatp1* by 4.2-fold (*P* = 0.003, Fig. 5*B*), and *mrp2* by 30-fold (*P* = 0.001, Fig. 5*C*) in AdHNF6-SV40SM cells.

The net effects of AdHNF6 infection of higher *HNF6*, *Foxa2*, *HNF1a*, and *HNF4a* expression in AdHNF6-SV40SM relative to AdHNF6-SV40LG were associated with correspondingly higher levels of *ntcp* (2.4-fold, *P* = 0.02), *oatp1*

Table 2. *Effect of AdHNF6 on HNF6 and HNF6 target genes*

	AdLacZ	AdH6	x-Fold AdHNF6 vs. AdLacZ	x-fold AdHNF6 SV40SM vs. AdHNF6 SV40LG	P Value
HNF6					
SV40LG	0.7 ± 0.3	725 ± 109	1,450		
SV40SM	0.4 ± 0.3	1043 ± 98	2,608	1.4	0.02
GK					
SV40LG	0.8 ± 0.37	13 ± 1.9	16		
SV40SM	0.6 ± 0.2	23 ± 4.6	38	1.8	0.02
TGFb2R					
SV40LG	1 ± 0.14	0.8 ± 0.1	0.8		
SV40SM	1 ± 0.11	0.5 ± 00.1	2.0	1.6	0.03

SV40LG and SV40SM cells were treated with AdLacZ or AdHNF6 for 24 h. Total RNA was extracted for real-time PCR analysis of *HNF6, cyclophilin,* and HNF6-target genes *glucokinase (GK)* and *TGFb2R*. Table shows gene levels after normalizing with housekeeping gene *cyclophilin*, the x-fold changes in gene level between AdLacZ-treated cells and AdHNF6-treated cells, and the x-fold difference between AdHNF6-treated SV40SM and AdHNF6-treated SV40LG cells with its corresponding *P* values. See text for definitions of gene acronyms.
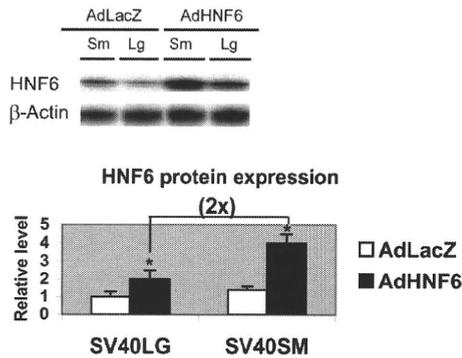
Fig. 3. Effect of adenoviral HNF6 (AdHNF6) treatment on SV40 biliary epithelial cell (BEC) HNF6 protein expression. SV40LG and SV40SM cells were infected with AdLacZ and AdHNF6 for 24 h. Micrograph shows Western blotting results of HNF6 protein expression in SV40SM (Sm) and SV40LG (Lg) cells. Bar graph shows densitometry results of the immune complexes after normalization to β-actin with values reported relative to AdHNF6-infected SV40LG cells, showing a twofold higher HNF6 expression in AdHNF6-SV40SM over AdHNF6-SV40LG cells. *Significant P values.

(3.4-fold, $P = 0.006$), and $mrp2$ (2.5-fold, $P = 0.02$) in AdHNF6-SV40SM compared with AdHNF6-SV40LG cells.

Effects of increasing in vivo HNF6 expression on target gene transcription. To evaluate HNF6 in vivo target gene transcriptional response, hepatic HNF6 expression was physiologically enhanced by treatment with recombinant GH, a known STAT5-mediated transcriptional activator of HNF6 promoter (21). The *mrp2* gene expression was selected since, among the above bile transport gene-positive transcriptional responses to AdHNF6 treatment, *mrp2* levels were the most dramatically enhanced (by >20-fold in both SV40LG and SV40SM cells). Large and small BEC were isolated for gene expression analyses following 24 h of GH administration (Fig. 6). As expected from our laboratory's previous work in GH-treated liver (40, 41), *HNF6* gene expression was appropriately increased in large (by 1.5-

fold) and small BEC (by 1.7-fold) relative to PBS control (Fig. 6A). Consistent with our laboratory's previous findings that SV40SM cell lines displayed a magnified responsiveness to HNF6 induction relative to SV40LG cells, in vivo GH-treated small BEC had significant increases of *glucokinase* (2.8-fold, $P = 0.05$; Fig. 6B) and *mrp2* (5-fold, $P < 0.001$; Fig. 6A) gene expression over PBS-treated small BEC. Of note, unlike our laboratory's previous SV40 cell data showing enhanced *glucokinase* (Table 1) and *mrp2* response (Fig. 5C) to AdHNF6 infection in SV40LG cells, this increase was not seen in GH-treated large BEC, possibly because GH-induced *HNF6* in vivo expression was less dramatic. Compared with GH-treated large BEC, *glucokinase* and *mrp2* levels were 2.4-fold ($P = 0.04$) and 3.4-fold ($P < 0.001$), respectively, higher in GH-treated small BEC than GH-treated large BEC, showing that the same pattern of small BEC in vitro sensitivity in its transcriptional response to HNF6 was also seen in vivo.

DISCUSSION

The concept of biliary cell morphological and functional heterogeneity originating from the early work in rat biliary model system (2, 6) has progressively gained acceptance with many comprehensive reviews on this subject (14, 19, 28). Since the liver epithelial cell phenotype and function are determined by the spectrum of hepatic-specific genes, whose expression are regulated by liver-enriched HNFs, an evaluation of the BEC transcriptional characteristics is a logical start in furthering our understanding of basic molecular mechanism for BEC diversities.

We found that the small and large BEC display distinctive constitutive levels of hepatocyte transcription factors and biliary cell-enriched gene expression. The small SV40 BEC exhibited higher expression of *Foxa2*, *HNF1a*, and *HNF4a* hepatocyte transcription factors. This transcriptional profile likely provides the molecular basis for higher constitutive expression of HNF1a-, HNF4a-, and Foxa2-candidate target genes such as *ntcp*, *oatp1*, and *mrp2* in SV40SM cells. The

A

	Cells	Cells	x-fold gene levels	
Genes	**AdHNF6 SV40LG**	**AdHNF6 SV40SM**	**SV40SM over SV40LG**	**p value**
HNF1a	1 +/- 0.2	15 +/- 2.5	15*	0.001
HNF4a	2 +/- 0.38	13 +/- 6	6.5*	0.03
Foxa2	0.2+/- 0.04	0.8 +/- 0.1	4*	0.01

B

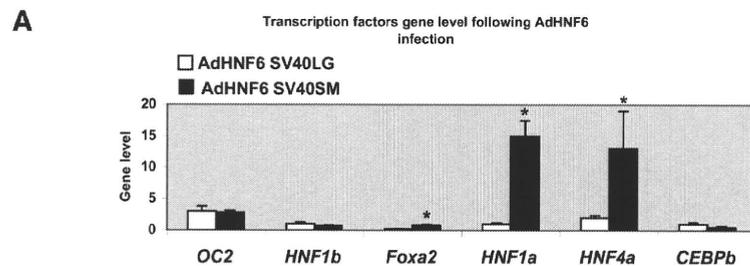| *HNF4a*	**AdLacZ**	**AdHNF6**	**x-fold suppression**	**p value**
SV40 LG	11.8 +/- 1.3	2 +/- 0.38	6.4*	0.002
SV40 SM	31 +/- 7.2	13 +/- 6	2*	0.05

Fig. 4. Net effect of AdHNF6 treatment on SV40 BEC hepatocyte nuclear factor (HNF) expression. A: bar graph shows *OC2*, *HNF1b*, *Foxa2*, *HNF1a*, *HNF4a*, and *C/EBPb* gene levels for AdHNF6-infected SV40LG and AdHNF6-infected SV40SM cells. *Significant differences in levels between AdHNF6 SV40LG vs. AdHNF6 SV40SM cells. Table shows gene levels and the x-fold higher expression levels of *HNF1*, *HNF4a*, and *Foxa2* in AdHNF6-SV40SM relative to AdHNF6-SV40LG cells with the corresponding P values. B: table shows *HNF4a* gene levels in AdLacZ- and AdHNF6-infected SV40LG and SV40SM cells and x-fold suppression (with the corresponding P values) in gene levels of AdHNF6-infected SV40 cells relative to AdLacZ-infected cells. *Significant differences in levels between AdLacZ and AdHNF6-infected cells.

A

Ntcp gene expression

(2.4x)

□ AdLacZ
■ AdHNF6

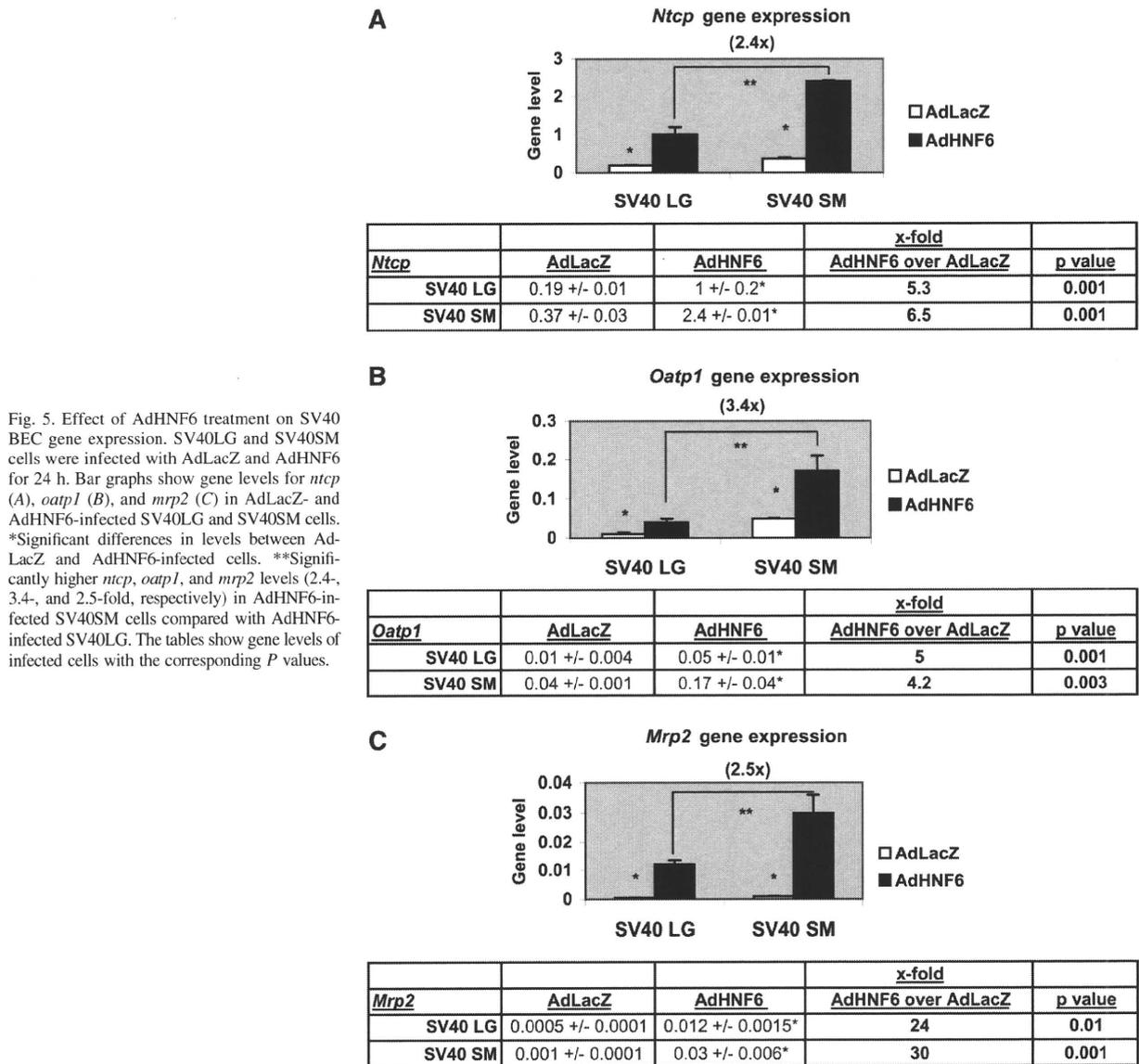| Ntcp	AdLacZ	AdHNF6	x-fold AdHNF6 over AdLacZ	p value
SV40 LG	0.19 +/- 0.01	1 +/- 0.2*	5.3	0.001
SV40 SM	0.37 +/- 0.03	2.4 +/- 0.01*	6.5	0.001

Fig. 5. Effect of AdHNF6 treatment on SV40 BEC gene expression. SV40LG and SV40SM cells were infected with AdLacZ and AdHNF6 for 24 h. Bar graphs show gene levels for *ntcp* (*A*), *oatp1* (*B*), and *mrp2* (*C*) in AdLacZ- and AdHNF6-infected SV40LG and SV40SM cells. *Significant differences in levels between Ad-LacZ and AdHNF6-infected cells. **Significantly higher *ntcp*, *oatp1*, and *mrp2* levels (2.4-, 3.4-, and 2.5-fold, respectively) in AdHNF6-infected SV40SM cells compared with AdHNF6-infected SV40LG. The tables show gene levels of infected cells with the corresponding *P* values.

B

Oatp1 gene expression

(3.4x)

□ AdLacZ
■ AdHNF6

Oatp1	AdLacZ	AdHNF6	x-fold AdHNF6 over AdLacZ	p value
SV40 LG	0.01 +/- 0.004	0.05 +/- 0.01*	5	0.001
SV40 SM	0.04 +/- 0.001	0.17 +/- 0.04*	4.2	0.003

C

Mrp2 gene expression

(2.5x)

□ AdLacZ
■ AdHNF6

Mrp2	AdLacZ	AdHNF6	x-fold AdHNF6 over AdLacZ	p value
SV40 LG	0.0005 +/- 0.0001	0.012 +/- 0.0015*	24	0.01
SV40 SM	0.001 +/- 0.0001	0.03 +/- 0.006*	30	0.001

dominance of *HNF1a* and *HNF4a* as BEC-enriched transcription factors in small biliary cells is consistent with previous genomewide promoter analyses of human hepatocytes, showing that *HNF1a*, *HNF4a*, and *HNF6* are the core group of HNFs in orchestrating the transcription of a wide array of differentiated hepatic genes (29). Of great interest to us, it remains to be seen in future experiments whether large biliary cell could be induced into acquiring the same small BEC molecular repertoire upon enforced expression of these HNF1a-, HNF4a-, and Foxa2-enriched hepatocyte transcription factors, and, conversely, whether the small biliary cell would lose its constitutive molecular imprint following reversal of its HNF profile.

Small BEC also displayed a higher transcriptional response level to HNF6 treatment. Since HNF6 transcriptional

regulation of target gene also involves other HNF, such as *HNF4a* (21), *HNF1b* (9), and *Foxa2* (21), we first evaluated HNF response patterns to AdHNF6 in SV40 BEC. Consistent with the known cross-regulatory transcriptional network among HNFs, AdHNF6 treatment affected the HNF profile of BEC, albeit with a negative effect on *HNF4a* transcription for both large and small SV40 BECs. A simple explanation for this unexpected suppressive response is that previous results demonstrating hepatic HNF4a-positive transcriptional response to HNF6 could not be extrapolated to that of BEC. Alternatively, the approach of using HNF6 adenoviral expression vectors to transduce HNF6 expression in BEC cell lines limits this analysis to HNFs as cell-autonomous regulators outside the context of in vivo systems. An evaluation of in vivo cholangiocytes' HNF and
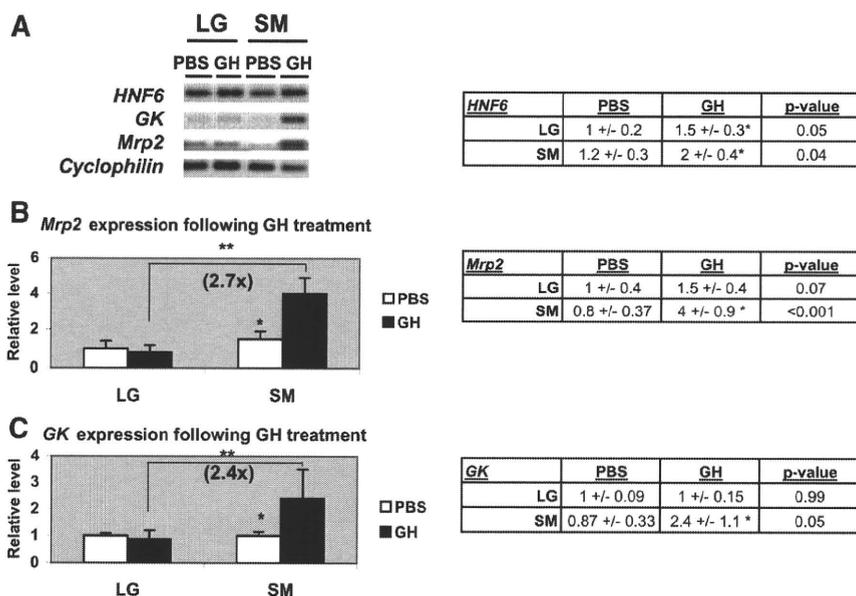
A

HNF6	PBS	GH	p-value
LG	1 +/- 0.2	1.5 +/- 0.3*	0.05
SM	1.2 +/- 0.3	2 +/- 0.4*	0.04

B Mrp2 expression following GH treatment

Mrp2	PBS	GH	p-value
LG	1 +/- 0.4	1.5 +/- 0.4	0.07
SM	0.8 +/- 0.37	4 +/- 0.9 *	<0.001

C GK expression following GH treatment

GK	PBS	GH	p-value
LG	1 +/- 0.09	1 +/- 0.15	0.99
SM	0.87 +/- 0.33	2.4 +/- 1.1 *	0.05

Fig. 6. Effects of growth hormone (GH)-mediated *HNF6* increases on BEC gene expression. LG and SM BEC were isolated from PBS- or GH-treated mice (*n* = 3). Total RNA was extracted for real-time PCR analyses of *HNF6*, *mrp2*, *GK*, and *cyclophilin*. *A*: micrograph shows representative real-time PCR gel results, and table shows *HNF6* gene levels with the corresponding *P* values. *B* and *C*: bar graphs show gene levels for *mrp2* (*B*) and *GK* (*C*) in PBS- and GH-treated BEC. *Significant differences in levels between PBS- vs. GH-treated BEC. **Significantly higher *mrp2* and *GK* levels (2.7- and 2.4-fold, respectively) in GH-treated SM relative to LG cholangiocytes. Tables show the gene levels with the corresponding *P* values.

target gene response are pending to shed light on the true physiological significance of these in vitro findings. The relevance of the suppressive transcriptional response of HNF4a to HNF6 overexpression in SV40BEC is unclear, but does not diminish the remarkable findings that Foxa2, HNF1a, and HNF4a remain dominant transcription factors in the AdHNF6-infected small BEC, with commensurate higher expression levels of their target genes, *ntcp*, *oatp1*, and *mrp2*.

Following AdHNF6 infection, despite unchanged *Foxa2* and *HNF1a*, yet suppressed *HNF4a* expression, *HNF1a-*, *HNF4a-*, and/or *Foxa2* target gene *ntcp*, *oatp1*, and *mrp2* levels were significantly enhanced in both large and small SV40 cells, suggesting that the response pattern of these bile transport genes is more complex than just straightforward transcriptional regulation by *HNF1a*, *HNF4*, *Foxa2*, or *HNF6*, since HNFs commonly function in a cross-regulatory fashion. With respect to *ntcp*, transient transfection of CMV-HNF6 expression vectors in HepG2 cell lines did not activate *ntcp* reporter gene constructs (data not shown). Furthermore, prior AdHNF6 liver infection by tail vein injection did not enhance whole liver *ntcp* or *mrp2* expression (40), suggesting that *ntcp* and *mrp2* gene response cannot be directly attributed to simple HNF6 transcriptional effects on their promoters. Since HNF commonly participate in a transcriptional network with the proper complement of HNF and cross-interaction among HNFs controlling the target gene profile, BEC upregulation of *ntcp* and *mrp2* expression following AdHNF6 infection could be due to potential molecular synergistic interactions between HNF6 and HNF1a/HNF4a/Foxa2, perhaps through the recruitment of coactivators to orchestrate target gene activation. A precedence for this mechanism has been described with HNF6-HNF4a activation of *glucose-6-phosphatase* promoter by joint engagement of the peroxisome proliferator-activated receptor-γ coactivator-1α (5); or with HNF6-C/EBPa recruitment of the CREB binding protein CBP coac-

tivator to enhance *Foxa2* promoter activities (33, 42). Of note, *oatp1* hepatic gene expression and *oatp1* promoter occupancy by HNF6 nuclear proteins are severely diminished in HNF6 liver conditional null mice (manuscript submitted), suggesting that *oatp1* is an authentic HNF6 target gene. Upregulation of *oatp1* expression in AdHNF6 treated cells is consistent with direct transcriptional stimulation of *oatp1* by HNF6 or HNF1a-HNF6 interaction.

Gene profiling (12, 38) and functional studies (14) have shown that large BEC participate in choleresis, immune, and hormone regulation. Our gene expression data suggest that small BEC may carry a more substantial role in the transport of bile acid and bile acid constituents than large BEC. Further analyses for the respective contribution of these cell populations to the liver adaptive response to injury in experimental models of cholestasis are pending to assess the physiological significance of these observations.

Overall, the results lend support to our hypothesis that the large and small cholangiocytes have different transcriptional characteristics, thus providing a potential mechanistic basis for their functional heterogeneity. The data also imply that the well-described intricate interactions among hepatocyte transcription factors in coordinating the transcriptional profile of end genes in hepatocytes may also exist in BECs. Further characterization of the complexities of promoter regulation of biliary-enriched genes in the large and small BECs will enhance our understanding of their differential susceptibility to disease processes in an effort toward modulating their individual pathological responses.

DISCLOSURES

No conflicts of interest, financial or otherwise, are declared by the author(s).

REFERENCES

1. **Alpini G, Glaser S, Robertson W, Phinizy JL, Rodgers RE, Caligiuri A, LeSage G.** Bile acids stimulate proliferative and secretory events in large but not small cholangiocytes. *Am J Physiol Gastrointest Liver Physiol* 273: G518–G529, 1997.
2. **Alpini G, Prall RT, LaRusso NF.** The pathobiology of biliary epithelia. In: *The Liver; Biology & Pathobiology,* edited by Arias IM, Boyer JL, Chisari FV, Fausto N, Jakoby W, Schachter D, and Shafritz DA. Philadelphia, PA: Lippincott Williams & Wilkins, 2001, p. 421–435.
3. **Alpini G, Roberts S, Kuntz SM, Ueno Y, Gubba S, Podila PV, LeSage G, LaRusso NF.** Morphological, molecular, and functional heterogeneity of cholangiocytes from normal rat liver. *Gastroenterology* 110: 1636–1643, 1996.
4. **Andrejko KM, Raj NR, Kim PK, Cereda M, Deutschman CS.** IL-6 modulates sepsis-induced decreases in transcription of hepatic organic anion and bile acid transporters. *Shock* 29: 490–496, 2008.
5. **Beaudry JB, Pierreux CE, Hayhurst GP, Plumb-Rudewiez N, Weiss MC, Rousseau GG, Lemaigre FP.** Threshold levels of hepatocyte nuclear factor 6 (HNF-6) acting in synergy with HNF-4 and PGC-1alpha are required for time-specific gene expression during liver development. *Mol Cell Biol* 26: 6037–6046, 2006.
6. **Benedetti A, Bassotti C, Rapino K, Marucci L, Jezequel AM.** A morphometric study of the epithelium lining the rat intrahepatic biliary tree. *J Hepatol* 24: 335–342, 1996.
7. **Bochkis IM, Rubins NE, White P, Furth EE, Friedman JR, Kaestner KH.** Hepatocyte-specific ablation of Foxa2 alters bile acid homeostasis and results in endoplasmic reticulum stress. *Nat Med* 14: 828–836, 2008.
8. **Clotman F, Jacquemin P, Plumb-Rudewiez N, Pierreux CE, Van der Smissen P, Dietz HC, Courtoy PJ, Rousseau GG, Lemaigre FP.** Control of liver cell fate decision by a gradient of TGF beta signaling modulated by Onecut transcription factors. *Genes Dev* 19: 1849–1854, 2005.
9. **Clotman F, Lannoy VJ, Reber M, Cereghini S, Cassiman D, Jacquemin P, Roskams T, Rousseau GG, Lemaigre FP.** The onecut transcription factor HNF6 is required for normal development of the biliary tract. *Development* 129: 1819–1828, 2002.
10. **Costa RH, Kalinichenko VV, Holterman AX, Wang X.** Transcription factors in liver development, differentiation, and regeneration. *Hepatology* 38: 1331–1347, 2003.
11. **Dietrich CG, Martin IV, Porn AC, Voigt S, Gartung C, Trautwein C, Geier A.** Fasting induces basolateral uptake transporters of the SLC family in the liver via HNF4alpha and PGC1alpha. *Am J Physiol Gastrointest Liver Physiol* 293: G585–G590, 2007.
12. **Fukushima K, Ueno Y.** Bioinformatic approach for understanding the heterogeneity of cholangiocytes. *World J Gastroenterol* 12: 3481–3486, 2006.
13. **Geier A, Martin IV, Dietrich CG, Balasubramaniyan N, Strauch S, Suchy FJ, Gartung C, Trautwein C, Ananthanarayanan M.** Hepatocyte nuclear factor-4alpha is a central transactivator of the mouse Ntcp gene. *Am J Physiol Gastrointest Liver Physiol* 295: G226–G233, 2008.
14. **Glaser S, Francis H, Demorrow S, Lesage G, Fava G, Marzioni M, Venter J, Alpini G.** Heterogeneity of the intrahepatic biliary epithelium. *World J Gastroenterol* 12: 3523–3536, 2006.
15. **Glaser SS, Gaudio E, Rao A, Pierce LM, Onori P, Franchitto A, Francis HL, Dostal DE, Venter JK, DeMorrow S, Mancinelli R, Carpino G, Alvaro D, Kopriva SE, Savage JM, Alpini GD.** Morphological and functional heterogeneity of the mouse intrahepatic biliary epithelium. *Lab Invest* 89: 456–469, 2009.
16. **Hayhurst GP, Lee YH, Lambert G, Ward JM, Gonzalez FJ.** Hepatocyte nuclear factor 4alpha (nuclear receptor 2A1) is essential for maintenance of hepatic gene expression and lipid homeostasis. *Mol Cell Biol* 21: 1393–1403, 2001.
17. **Holterman AX, Tan Y, Kim W, Yoo KW, Costa RH.** Diminished hepatic expression of the HNF-6 transcription factor during bile duct obstruction. *Hepatology* 35: 1392–1399, 2002.
18. **Jacquemin P, Lannoy VJ, Rousseau GG, Lemaigre FP.** OC-2, a novel mammalian member of the ONECUT class of homeodomain transcription factors whose function in liver partially overlaps with that of hepatocyte nuclear factor-6. *J Biol Chem* 274: 2665–2671, 1999.
19. **Kanno N, LeSage G, Glaser S, Alvaro D, Alpini G.** Functional heterogeneity of the intrahepatic biliary epithelium. *Hepatology* 31: 555–561, 2000.
20. **Kitanaka S, Sato U, Igarashi T.** Regulation of human insulin, IGF-I, and multidrug resistance protein 2 promoter activity by hepatocyte nuclear factor (HNF)-1beta and HNF-1alpha and the abnormality of HNF-1beta mutants. *J Endocrinol* 192: 141–147, 2007.
21. **Lahuna O, Rastegar M, Maiter D, Thissen JP, Lemaigre FP, Rousseau GG.** Involvement of STAT5 (signal transducer and activator of transcription 5) and HNF-4 (hepatocyte nuclear factor 4) in the transcriptional control of the hnf6 gene by growth hormone. *Mol Endocrinol* 14: 285–294, 2000.
22. **Lannoy VJ, Decaux JF, Pierreux CE, Lemaigre FP, Rousseau GG.** Liver glucokinase gene expression is controlled by the onecut transcription factor hepatocyte nuclear factor-6. *Diabetologia* 45: 1136–1141, 2002.
23. **Lazaridis KN, Strazzabosco M, Larusso NF.** The cholangiopathies: disorders of biliary epithelia. *Gastroenterology* 127: 1565–1577, 2004.
24. **Lee CS, Friedman JR, Fulmer JT, Kaestner KH.** The initiation of liver development is dependent on Foxa transcription factors. *Nature* 435: 944–947, 2005.
25. **Lee YH, Magnuson MA, Muppala V, Chen SS.** Liver-specific reactivation of the inactivated Hnf-1alpha gene: elimination of liver dysfunction to establish a mouse MODY3 model. *Mol Cell Biol* 23: 923–932, 2003.
26. **Liu JJ, Glickman JN, Masyuk AI, Larusso NF.** Cholangiocyte bile salt transporters in cholesterol gallstone-susceptible and resistant inbred mouse strains. *J Gastroenterol Hepatol* 23: 1596–1602, 2008.
27. **Maher JM, Slitt AL, Callaghan TN, Cheng X, Cheung C, Gonzalez FJ, Klaassen CD.** Alterations in transporter expression in liver, kidney, and duodenum after targeted disruption of the transcription factor HNF1alpha. *Biochem Pharmacol* 72: 512–522, 2006.
28. **Marzioni M, Glaser SS, Francis H, Phinizy JL, LeSage G, Alpini G.** Functional heterogeneity of cholangiocytes. *Semin Liver Dis* 22: 227–240, 2002.
29. **Odom DT, Zizlsperger N, Gordon DB, Bell GW, Rinaldi NJ, Murray HL, Volkert TL, Schreiber J, Rolfe PA, Gifford DK, Fraenkel E, Bell GI, Young RA.** Control of pancreas and liver gene expression by HNF transcription factors. *Science* 303: 1378–1381, 2004.
30. **Parviz F, Matullo C, Garrison WD, Savatski L, Adamson JW, Ning G, Kaestner KH, Rossi JM, Zaret KS, Duncan SA.** Hepatocyte nuclear factor 4alpha controls the development of a hepatic epithelium and liver morphogenesis. *Nat Genet* 34: 292–296, 2003.
31. **Plumb-Rudewiez N, Clotman F, Strick-Marchand H, Pierreux CE, Weiss MC, Rousseau GG, Lemaigre FP.** Transcription factor HNF-6/OC-1 inhibits the stimulation of the HNF-3alpha/Foxa1 gene by TGF-beta in mouse liver. *Hepatology* 40: 1266–1274, 2004.
32. **Qadri I, Hu LJ, Iwahashi M, Al-Zuabi S, Quattrochi LC, Simon FR.** Interaction of hepatocyte nuclear factors in transcriptional regulation of tissue specific hormonal expression of human multidrug resistance-associated protein 2 (abcc2). *Toxicol Appl Pharmacol* 234: 281–292, 2009.
33. **Rausa FM 3rd, Hughes DE, Costa RH.** Stability of the hepatocyte nuclear factor 6 transcription factor requires acetylation by the CREB-binding protein coactivator. *J Biol Chem* 279: 43070–43076, 2004.
34. **Raynaud P, Carpentier R, Antoniou A, Lemaigre FP.** Biliary differentiation and bile duct morphogenesis in development and disease. *Int J Biochem Cell Biol.* In press.
35. **Samadani U, Costa RH.** The transcriptional activator hepatocyte nuclear factor 6 regulates liver gene expression. *Mol Cell Biol* 16: 6273–6284, 1996.
36. **Schrem H, Klempnauer J, Borlak J.** Liver-enriched transcription factors in liver function and development. I. The hepatocyte nuclear factor network and liver-specific gene expression. *Pharmacol Rev* 54: 129–158, 2002.
37. **Strazzabosco M, Fabris L, Spirli C.** Pathophysiology of cholangiopathies. *J Clin Gastroenterol* 39: S90–S102, 2005.
38. **Ueno Y, Alpini G, Yahagi K, Kanno N, Moritoki Y, Fukushima K, Glaser S, LeSage G, Shimosegawa T.** Evaluation of differential gene expression by microarray analysis in small and large cholangiocytes isolated from normal mice. *Liver Int* 23: 449–459, 2003.
39. **Velho G, Froguel P.** Maturity-onset diabetes of the young (MODY), MODY genes and non-insulin-dependent diabetes mellitus. *Diabetes Met* 23, *Suppl* 2: 34–37, 1997.

40. **Wang M, Chen M, Zheng G, Dillard B, Tallarico M, Ortiz Z, Holterman AX.** Transcriptional activation by growth hormone of HNF-6-regulated hepatic genes, a potential mechanism for improved liver repair during biliary injury in mice. *Am J Physiol Gastrointest Liver Physiol* 295: G357–G366, 2008.

41. **Wang M, Tan Y, Costa RH, Holterman AX.** In vivo regulation of murine CYP7A1 by HNF-6: a novel mechanism for diminished CYP7A1 expression in biliary obstruction. *Hepatology* 40: 600–608, 2004.

42. **Yoshida Y, Hughes DE, Rausa FM 3rd, Kim IM, Tan Y, Darlington GJ, Costa RH.** C/EBPalpha and HNF6 protein complex formation stimulates HNF6-dependent transcription by CBP coactivator recruitment in HepG2 cells. *Hepatology* 43: 276–286, 2006.

– 377 –

Knockout of Secretin Receptor Reduces Large Cholangiocyte Hyperplasia in Mice With Extrahepatic Cholestasis Induced by Bile Duct Ligation

Shannon Glaser,[2,4]* Ian P. Lam,[6]* Antonio Franchitto,[5] Eugenio Gaudio,[5] Paolo Onori,[7] Billy K. Chow,[6] Candace Wise,[2,3,4] Shelley Kopriva,[2,4] Julie Venter,[2,4] Mellanie White,[2,4] Yoshiyuki Ueno,[9] David Dostal,[4] Guido Carpino,[8] Romina Mancinelli,[4,5] Wendy Butler,[1] Valorie Chiasson,[4] Sharon DeMorrow,[2,4] Heather Francis,[2,3,4] and Gianfranco Alpini[1,2,4]

During bile duct ligation (BDL), the growth of large cholangiocytes is regulated by the cyclic adenosine monophosphate (cAMP)/extracellular signal-regulated kinase 1/2 (ERK1/2) pathway and is closely associated with increased secretin receptor (SR) expression. Although it has been suggested that SR modulates cholangiocyte growth, direct evidence for secretin-dependent proliferation is lacking. SR wild-type (WT) ($SR^{+/+}$) or SR knock-out ($SR^{-/-}$) mice underwent sham surgery or BDL for 3 or 7 days. We evaluated SR expression, cholangiocyte proliferation, and apoptosis in liver sections and proliferating cell nuclear antigen (PCNA) protein expression and ERK1/2 phosphorylation in purified large cholangiocytes from WT and $SR^{-/-}$ BDL mice. Normal WT mice were treated with secretin (2.5 nmoles/kg/day by way of osmotic minipumps for 1 week), and biliary mass was evaluated. Small and large cholangiocytes were used to evaluate the *in vitro* effect of secretin (100 nM) on proliferation, protein kinase A (PKA) activity, and ERK1/2 phosphorylation. SR expression was also stably knocked down by short hairpin RNA, and basal and secretin-stimulated cAMP levels (a functional index of biliary growth) and proliferation were determined. SR was expressed by large cholangiocytes. Knockout of SR significantly decreased large cholangiocyte growth induced by BDL, which was associated with enhanced apoptosis. PCNA expression and ERK1/2 phosphorylation were decreased in large cholangiocytes from $SR^{-/-}$ BDL compared with WT BDL mice. *In vivo* administration of secretin to normal WT mice increased ductal mass. *In vitro*, secretin increased proliferation, PKA activity, and ERK1/2 phosphorylation of large cholangiocytes that was blocked by PKA and mitogen-activated protein kinase kinase inhibitors. Stable knockdown of SR expression reduced basal cholangiocyte proliferation. SR is an important trophic regulator sustaining biliary growth. *Conclusion:* The current study provides strong support for the potential use of secretin as a therapy for ductopenic liver diseases. (HEPATOLOGY 2010;52:204-214)

Cholangiocytes line the intrahepatic biliary system, which modifies the bile of canalicular origin into its final composition before reaching the small intestine.[1,2] Several gastrointestinal peptides/hormones, including bombesin, gastrin, and secretin, regulate cholangiocyte secretory activity.[1-3] Among these factors, secretin plays a key role in the biliary secretion of water and bicarbonate, because secretin receptor (SR) is expressed in rodent and human liver by larger bile ducts.[1,4-6] In large cholangiocytes, secretin

204

increases cyclic adenosine monophosphate (cAMP) levels[1,4,5,7,8] and induces the opening of the Cl^- channel (cystic fibrosis transmembrane conductance regulator, CFTR)[9] leading to the activation of the Cl^-/HCO_3^- anion exchanger 2[10] and secretion of bicarbonate in bile.[2,3]

Human cholangiocytes are the target cells in several cholangiopathies, including primary biliary cirrhosis and primary sclerosing cholangitis, diseases associated with dysregulation of the balance between cholangiocyte proliferation/apoptosis.[11] Rodent cholangiocytes, which are normally mitotically quiescent,[12,13] markedly proliferate in animal models of cholestasis including extrahepatic bile duct ligation (BDL) or acute carbon tetrachloride (CCl_4) administration.[12,14] The proliferative response of the intrahepatic biliary epithelium to BDL is heterogeneous, because large (but not small) cholangiocytes proliferate through the activation of cAMP-dependent ERK1/2 signaling[12,15] leading to enhanced ductal mass.[5,12,14]

Because SR is only expressed by large cholangiocytes in the liver,[1,4,5,9,12,14] changes in the functional expression of this receptor have been suggested as a pathophysiological tool for evaluating changes in the degree of cholangiocyte growth/loss.[5,12,14] Indeed, we have shown that (1) cholangiocyte hyperplasia (after BDL or 70% hepatectomy) is associated with enhanced SR expression and secretin-stimulated cAMP levels and bicarbonate secretion[12,13,16-18] and (2) cholangiocyte damage (after CCl_4) decreases the functional expression of SR in large cholangiocytes.[14] In pathological conditions—such as the CCl_4 model, which is characterized by lack or damage of the hormonally responsive large cholangiocytes—small cholangiocytes proliferate and express SR de novo.[14]

The hormonal actions of secretin through SR have been studied in the pancreas, stomach, and biliary epithelium.[19] Although it has been suggested that SR modulates cholangiocyte growth,[2,12-14] the direct link between SR expression and its possible role in the regulation of biliary proliferation has not been elucidated. The aim of our study was to determine the role that

SR plays in sustaining large cholangiocyte growth during cholestasis induced by BDL.

Materials and Methods

Materials. Reagents were purchased from Sigma Chemical Co. (St. Louis, MO) unless otherwise stated. The nuclear dye 4′,6-diamidino-2-phenylindole was obtained from Molecular Probes, Inc. (Eugene, OR). Porcine secretin was purchased from Peninsula Laboratories (Belmont, CA). The polyclonal SR antibody (Santa Cruz Biotechnology, Santa Cruz, CA) was raised against a peptide mapping at the C terminus of SR of human origin and cross-reacts with mouse.[20] The antibody against proliferating cell nuclear antigen (PCNA) was purchased from Santa Cruz Biotechnology. The mouse anti–cytokeratin-19 antibody was purchased from Caltag Laboratories Inc. (Burlingame, CA). Goat phosphorylated ERK1/2 and total ERK1/2 (44-42 kDa) polyclonal affinity purified antibodies were purchased from Santa Cruz Biotechnology. The RIA kits for the determination of intracellular cAMP levels in cholangiocytes were purchased from Perkin Elmer (Shelton, CT).

Animal Models. All animal experiments (Table 1) were performed in accordance with a protocol approved by the Scott & White and Texas A&M Health Science Center Institutional Animal Care and Use Committee and conformed to the Guide for the Care and Use of Laboratory Animals published by the National Institutes of Health (Publication No. 85-23, revised 1996). Our $SR^{+/+}$ (wild-type [WT]) or SR knockout ($SR^{-/-}$)[21] mice were maintained in a temperature-controlled environment (20-22°C) with a 12:12-hour light/dark cycle. We used adult male WT and $SR^{-/-}$ mice (approximately 25-30 g) of the N5 generation: (1) as normal treated with saline (0.9% NaCl) or secretin (2.5 nmol/kg/day, a dose similar to that used by us for another gastrointestinal hormone, gastrin, in rodents)[18] by way of intraperitoneally implanted Alzet osmotic minipumps (Alzet, CA) for 7

Address reprint requests to: Shannon Glaser, Ph.D., or Gianfranco Alpini Ph.D., Department of Medicine, Texas A&M Health Science Center, College of Medicine, Medical Research Building, 702 SW H. K. Dodgen Loop, Temple, TX 76504. E-mail: sglaser@medicine.tamhsc.edu(S. S.Glaser) Or galpini@medicine. tamhsc.edu (G. Alpini); fax: 254-724-5944.